Published in final edited form as:
Virology. 2009 January 20; 383(2): 348–361. doi:10.1016/j.virol.2008.09.030.

Chimeric human parainfluenza virus bearing the Ebola virus glycoprotein as the sole surface protein is immunogenic and highly protective against Ebola virus challenge

Alexander Bukreyev[a,*], **Andrea Marzi**[b], **Friederike Feldmann**[b], **Liqun Zhang**[d], **Lijuan Yang**[a], **Jerrold M. Ward**[a], **David W. Dorward**[e], **Raymond J. Pickles**[d], **Brian R. Murphy**[a], **Heinz Feldmann**[b,c], and **Peter L. Collins**[a]

a *National Institute of Allergy and Infectious Diseases, National Institutes of Health, Bethesda, Maryland, USA*

b *Special Pathogens Program, National Microbiology Laboratory, Canadian Science Centre for Human and Animal Health, Winnipeg, Canada*

c *Department of Medical Microbiology, University of Manitoba, Canada*

d *Cystic Fibrosis/Pulmonary Research and Treatment Center, University of North Carolina at Chapel Hill, Chapel Hill, North Carolina, USA*

e *Rocky Mountain Laboratories, National Institute of Allergy and Infectious Diseases, National Institutes of Health, Hamilton, Montana, USA*

Abstract

We generated a new live-attenuated vaccine against Ebola virus (EBOV) based on a chimeric virus HPIV3/ΔF-HN/EboGP that contains the EBOV glycoprotein (GP) as the sole transmembrane envelope protein combined with the internal proteins of human parainfluenza virus type 3 (HPIV3). Electron microscopy analysis of the virus particles showed that they have an envelope and surface spikes resembling those of EBOV and a particle size and shape resembling those of HPIV3. When HPIV3/ΔF-HN/EboGP was inoculated via apical surface of an in vitro model of human ciliated airway epithelium, the virus was released from the apical surface; when applied to basolateral surface, the virus infected basolateral cells but did not spread through the tissue. Following intranasal (IN) inoculation of guinea pigs, scattered infected cells were detected in the lungs by immunohistochemistry, but infectious HPIV3/ΔF-HN/EboGP could not be recovered from the lungs, blood, or other tissues. Despite the attenuation, the virus was highly immunogenic, and a single IN dose completely protected the animals against a highly lethal intraperitoneal challenge of guinea pig-adapted EBOV.

Introduction

Ebola virus (EBOV), along with the closely related Marburg virus, belongs to the family *Filoviridae* and causes sporadic outbreaks of hemorrhagic fever in Central Africa, with a

*Corresponding author: Building 50, Room 6505, NIAID, NIH, 50 South Dr. MSC 8007, Bethesda, MD 20892-8007 USA. Phone: 301-594-1854; fax: 301-496-8312; e-mail: abukreyev@nih.gov.

mortality rate of up to 88% (reviewed in Sanchez, Geisbert, and Feldmann, 2007). Multiple initial attempts to develop vaccines against EBOV were unsuccessful, suggesting that protective immunity against EBOV is not easily achievable. During the past decade, however, vector approaches for the development of vaccines against EBOV using adenoviruses, vesicular stomatitis virus (VSV), human parainfluenza type 3 (HPIV3), and Venezuelan equine encephalitis virus replicons have resulted in dramatic advances in vaccine development; nonetheless, no approved vaccine against EBOV exists so far (reviewed in Collins and Bukreyev, 2007). EBOV is transmitted by contact of infected fluids or tissues with mucosal membranes or breaks in the skin (Geisbert and Jahrling, 2004; Jaax et al., 1995; Jaax et al., 1996); in addition, infection has been demonstrated in non-human primates by aerosol administration of the virus (Johnson et al., 1995). Thus, the development of a vaccine that induces a strong local immune response in the respiratory tract in addition to systemic immunity would be advantageous.

We previously developed a topical respiratory tract vaccine against EBOV based on human parainfluenza virus type 3 (HPIV3), which is a common pediatric respiratory pathogen (reviewed in Karron and Collins, 2007). This involved modifying complete infectious HPIV3 by adding an additional transcription cassette expressing EBOV GP. The resulting virus, HPIV3/EboGP, efficiently infected guinea pigs and nonhuman primates, induced strong systemic and local immune responses in the respiratory tract, and conferred a high level of protection against an intraperitoneal (IP) challenge with EBOV (Bukreyev et al., 2007; Bukreyev et al., 2006). However, evaluation of various human adenovirus type 5 and vaccinia virus-vectored vaccines (Barouch et al., 2004; Casimiro et al., 2003; Fitzgerald et al., 2003; Kanesa-Thasan et al., 2000; Lemckert et al., 2005; Sharpe et al., 2001; Sumida et al., 2004; Zhi et al., 2006), including an adenovirus-vectored vaccine against EBOV (Yang et al., 2003), in animal models and in clinical studies demonstrated that preexisting immunity to the vector can abolish or greatly reduce the immunogenicity of the expressed foreign antigen. This also is a potential concern for an HPIV3-based vaccine, given the high seroprevalence for HPIV3 due to natural exposure. This concern has been somewhat ameliorated by the recent observation that, while the replication of HPIV3/EboGP indeed was strongly restricted in guinea pigs that had been previously infected with HPIV3, the immunogenicity of the EBOV GP insert was not greatly affected (Yang et al., 2008). However, it is not unusual for studies in small experimental animals to provide overly optimistic vaccine efficacy data, and these results remain to be confirmed in a non-human primate model (Geisbert et al., 2002). Thus, it would be useful to modify the HPIV3 vector to reduce its sensitivity to restriction by pre-existing immunity.

GP is the sole EBOV transmembrane envelope surface protein and mediates both attachment to cellular receptors and fusion of the viral envelope and the cellular plasma membrane (Sanchez, Geisbert, and Feldmann, 2007). In contrast, HPIV3 has two transmembrane envelope surface proteins, the hemagglutinin-neuraminidase (HN) that mediates receptor attachment, and the fusion protein (F) that is responsible for membrane fusion (Collins and Crowe, 2007). Since HPIV3 HN and F are the sole neutralization antigens of HPIV3, we explored the possibility of developing a chimeric virus that lacked HPIV3 HN and F and instead contained EBOV GP as the sole surface protein combined with the internal proteins of HPIV3. In the present study we report the successful recovery of such a chimeric virus, HPIV3/ΔF-HN/EboGP. We have characterized the viral particles by electron microscopy, confirmed the constellation of virion proteins expressed in infected cells, tested the ability of the virus to grow in various cell lines, determined the effect of HPIV3-specific neutralizing antibodies on growth in vitro, and tested the effect of GP on the polarity of vector infection in human ciliated airway epithelium (HAE). Finally, using the guinea pig model, we have determined the extent of virus replication, the organ distribution, and the immunogenicity and protective efficacy of this vaccine virus against EBOV challenge in vivo.

Results

Functional replacement of the HPIV3 HN and F proteins by EBOV GP as the sole surface protein

We previously constructed HPIV3/EboGP (Fig. 1A), in which complete recombinant HPIV3 was modified by insertion, between the P and M genes, of the coding sequence for EBOV GP flanked by HPIV3 gene-start (GS) and gene-end (GE) transcription signals (Bukreyev et al., 2007;Bukreyev et al., 2006). In the present study, HPIV3/EboGP was modified by deletion of the HPIV3 F and HN genes to create HPIV3/ΔF-HN/EboGP (Fig. 1A, B), which encodes full length EBOV GP (Sanchez et al., 1996;Volchkov et al., 1995) as the sole viral surface protein. Thus, infectivity of this chimeric virus would depend on incorporation of EBOV GP, which directs both attachment and fusion, into the particle. EBOV GP is a type I transmembrane protein that has an unusually short C-terminal cytoplasmic tail (CT) KFVF (Sanchez et al., 1993) that bears no sequence similarity to the much longer 23 amino acid C-terminal CT of the type I HPIV3 F protein (Spriggs et al., 1986), or the 31 amino acid N-terminal CT of the type II HPIV3 HN protein (Elango et al., 1986). The efficiency of incorporation of a foreign glycoprotein into a virus particle can be influenced by its CT, such that replacement of the foreign CT with that from an endogenous glycoprotein can increase incorporation (Tao et al., 2000). Therefore, we also designed a second virus, HPIV3/ΔF-HN/EboGPct, in which the CT of EBOV GP in HPIV3/ΔF-HN/EboGP was replaced with that of HPIV3 F protein (Fig. 1A, C). Both new chimeric constructs conformed to the “rule of six” (i.e., each genome length was an even multiple of six nucleotides), and both were designed so that the hexamer spacing of transcription signals was conserved (i.e., the first and last genes, N and L, initiate at the second hexamer nucleotide while all other genes initiate at the first hexamer nucleotide) (Kolakofsky et al., 1998).

The HPIV3/ΔF-HN/EboGP virus (expressing complete EBOV GP) was readily recoverable and viable. In contrast, while the HPIV3/ΔF-HN/EboGPct virus (expressing GP modified with the CT of HPIV3 F) was recoverable in multiple experiments as evidenced by clusters of rounded cells, it could not be amplified sufficient for its use in further experiments and will not be considered further. In the recovered, amplified HPIV3/ΔF-HN/EboGP virus, the regions that had been modified as well as the entire EBOV GP were amplified by RT-PCR and analyzed by sequencing, which confirmed the expected sequence and demonstrated a lack of adventitious mutations in these regions.

Analysis of HPIV3/ΔF-HN/EboGP particles

We purified HPIV3/ΔF-HN/EboGP and HPIV3 by ultracentrifugation in sucrose step gradients and compared the morphology of the virus particles by electron microscopy versus that of EBOV (Fig. 2). This showed that the overall size and the shape of the HPIV3/ΔF-HN/EboGP particles were similar to those of HPIV3; however, the envelope resembled that of EBOV both with regard to the appearance of the surface spikes (Sanchez, Geisbert, and Feldmann, 2007) and in being approximately 50% thinner than that of HPIV3.

Gradient-purified HPIV3/ΔF-HN/EboGP particles also were analyzed by gel electrophoresis under reducing and denaturing conditions followed by silver staining (Fig. 3A) or Western blot analysis an antiserum against EBOV GP (Fig. 3B). The silver-stained gel pattern of gradient-purified HPIV3/ΔF-HN/EboGP particles (Fig. 3A, lane 4) lacked the HN and F1 proteins, as expected, whereas these species were evident in preparations of HPIV3 and HPIV3/EboGP (lanes 2 and 3, respectively; note that the F1 band was much less visible for both HPIV3 and HPIV3/EboGP and was located close to an unidentified more abundant band). Analysis by silver staining (Fig. 3A) and Western blotting (Fig. 3B) also revealed the presence of EBOV GP, which migrated slightly above the 120 kDa marker band, in preparations of HPIV3/ΔF-

HN/EboGP (lane 4) and HPIV3/EboGP (lane 3), but not in the HPIV3 vector (lane 2). Importantly, in both assays the GP band was substantially denser in HPIV3/ΔF-HN/EboGP than in HPIV3/EboGP preparations: densitometer analysis of the silver stained gel showed that the GP:N ratio was 1.06 for HPIV3/ΔF-HN/EboGP compared to 0.66 for HPIV3/EboGP. The nearly two-fold greater incorporation of GP into the HPIV3/ΔF-HN/EboGP is likely attributable to the absence of the HPIV3 HN and F envelope proteins.

Growth of HPIV3/ΔF-HN/EboGP in cell culture monolayers

First, we compared the plaque size of HPIV3/ΔF-HN/EboGP with that of HPIV3 and HPIV3/EboGP. LLC-MK2 monkey kidney cells were infected with serial dilutions of the three viruses, covered with the medium containing 0.8% methylcellulose and incubated for 6 days at 32°C. Plaques were visualized by immunostaining with antibodies raised against purified HPIV3, in the case of HPIV3, or antibodies raised against purified, inactivated EBOV, in the case of HPIV3/ΔF-HN/EboGP and HPIV3/EboGP. The HPIV3/ΔF-HN/EboGP plaques were smaller than those of HPIV3, with an average diameter that was 36% that of the HPIV3 plaques (Fig. 4A), suggesting attenuation of the construct. The average diameter of plaques formed by HPIV3/EboGP was 62% of HPIV3 plaques. Similar results were obtained with Vero cells (not shown).

Unexpectedly, we found that HPIV3/ΔF-HN/EboGP formed plaques more readily than HPIV3 or HPIV3/EboGP. In LLC-MK2 cells, 1.0 $TCID_{50}$ of HPIV3 was found to be equivalent to 0.2 PFU, whereas 1.0 $TCID_{50}$ of HPIV3/ΔF-HN/EboGP was equivalent to 4.4 PFU, suggesting a 22-fold difference in the efficiency of plaque formation (for comparison, 1.0 $TCID_{50}$ of HPIV3/EboGP was equal to 0.6 PFU and thus more closely resembled HPIV3). Thus, replacement of the F and HN proteins with EBOV GP dramatically enhanced the ability of the virus to form plaques, although those plaques were reduced in size compared to those of HPIV3 and HPIV3/EboGP. The mechanistic basis for this effect is unknown. In all of the experiments in this report, titers and inocula were based on PFU, which amounts to 22-fold and 7.3-fold less HPIV3/ΔF-HN/EboGP relative to HPIV3 and HPIV3/EboGP, respectively, than had the titers and inocula been based on $TCID_{50}$. This provided for a conservative evaluation of the performance of this virus.

We then compared the growth kinetics of HPIV3/ΔF-HN/EboGP with those of HPIV3 and HPIV3/EboGP in monolayer cultures of LLC-MK2 and Vero monkey kidney cells and A549 human respiratory epithelial cells following infection with an input MOI 3 PFU/cell (Fig. 4B). In LLC-MK2 cells, the growth of HPIV3/ΔF-HN/EboGP was delayed compared with the other viruses but increased steadily such that, by day 6, the titer was high (8.7 $\log_{10}$ PFU/ml) and similar to that of HPIV3. In Vero cells, growth of HPIV3/ΔF-HN/EboGP was indistinguishable from that of HPIV3 and achieved a titer in excess of 7.0 $\log_{10}$ PFU/ml, whereas HPIV3/EboGP achieved a titer that was 10-fold higher under these conditions. Efficient replication in Vero cells is important because they are an approved substrate for the manufacture of vaccines for human use. In contrast, in human A549 cells, HPIV3/ΔF-HN/EboGP was severely attenuated compared to the other viruses and the titer never exceeded 6 $\log_{10}$ PFU/ml.

Infection using an in vitro model of human airway epithelium (HAE)

Next, we evaluated infection in an in vitro model of the human airway epithelium (HAE). This model consists of primary cells from clinical specimens that are grown and differentiated in vitro into a polarized, pseudostratified, ciliated epithelium that is morphologically and functionally similar to the epithelium of the conducting airways. HAE preparations from multiple donors were inoculated with HPIV3, HPIV3/EboGP (Bukreyev et al., 2006), or HPIV3/ΔF-HN/EboGP at an MOI of 2 PFU/cell via the apical or basolateral surface. We note that, due to the structure of these particular culture supports, inoculation of the basolateral

surface also exposed the apical surface to virus. At days 2 and 4 post inoculation, the cultures were fixed and viral antigens were detected in histological cross-sections using antibodies against virion preparations of HPIV3 (Fig. 5 B and C) or EBOV (Fig. 5, A, D and E). Following apical inoculation with HPIV3 (Fig. 5B, left side), mostly ciliated epithelial cells were positive for virus antigen, consistent with previous findings (Zhang et al., 2005). Loss of cilia and/or ciliated cells was noted by 4 days post-inoculation. Apical inoculation with HPIV3/EboGP (Fig. 5C and D, left side) also resulted in infected ciliated cells, although reduced in number. Based on analysis of multiple HAE, the mean percentages ± SE of infected ciliated cells following apical inoculation with HPIV3 or HPIV3/EboGP were as following: HPIV3, 83.3 ±7.1 (based on 5 preparations), and HPIV3/EboGP, 48.1±5.8 (based on 8 preparations), $P<0.01$. In contrast, apical infection with HPIV3/ΔF-HN/EboGP resulted in only rare isolated infected cells in the apical layer with no visible destruction of cells or cilia (Fig. 5E, left side).

Basolateral inoculation (which exposed both surfaces to virus) with HPIV3 did not detectably infect any basolateral cells, although numerous ciliated cells of the apical surface were infected (Fig. 5B, right side). Basolateral inoculation with HPIV3/EboGP (Fig. 5C and D, right side) showed the same pattern as for HPIV3, except that non-ciliated and non-apical cells (e.g., basal cells) also were occasionally infected (not shown), suggesting EBOV GP may increase HPIV3 tropism for basal or other non-ciliated cell-types. After basolateral infection with HPIV3/ΔF-HN/EboGP (Fig. 5E, right side), occasional infected individual or clusters of cells were detected located in apical, basolateral, and intermediate cell layers starting at day 4. These data indicate that all three viruses infected apical cells of HAE, with the order of efficiency being HPIV3>HPIV3/EboGP≫ HPIV3/ΔF-HN/EboGP, and that expression of EBOV GP conferred the ability to infect the basolateral and intermediate layers of HAE. However, infection via the apical surface never penetrated beyond the superficial cells.

Little or no HPIV3 antigen was detected in the cilia of infected cells using this particular polyvalent HPIV3-specific antiserum, although in a previous study using a monoclonal antibody specific to the HPIV3 F protein, expression was observed in the cilia (Zhang et al., 2005). This difference likely is a consequence of the use of different antibody preparations in the two studies. Interestingly, in the present study, cilia also were strongly stained with the anti-EBOV antibodies. Since GP is the only EBOV antigen expressed by HPIV3/ΔF-HN/EboGP, this specifically identified EBOV GP. The significance of this regional distribution of GP with regard to viral assembly and budding remains to be determined.

In separate experiments, triplicate HAE cultures per virus were inoculated via the apical or basolateral surface (the latter exposing both surfaces), and the kinetics of viral growth in HAE determined (Fig. 6). These experiments demonstrated that, following apical inoculation, all three viruses were detected in the apical compartment at all of the time points tested, although HPIV3/EboGP was somewhat attenuated compared to HPIV3, and HPIV3/ΔF-HN/EboGP was even further attenuated. This difference was generally consistent with the number of virus-positive cells that were observed on days 2 and 4 in the experiment shown in Fig. 5. In contrast, virus was not detected at the basolateral side following apical inoculation (not shown). When inoculation was by the basolateral route and samples were collected from the apical surface, the titers of HPIV3 and HPIV3/EboGP rapidly increased to high titers by day 3, indicative of robust viral replication and shedding from the apical surface, whereas replication and shedding of HPIV3/ΔF-HN/EboGP was barely detectable. These titers presumably reflect exposure of the apical cells to the viruses. With basolateral collection, intermediate viral titers (~ 4 $\log_{10}$ PFU/ml) were detected for each of the three viruses only on day 1, with little or no virus at later time points. We note that there are several aspects specific to inoculation of the basolateral surface that probably enhanced the retention of the initial inoculum at that surface, namely: the basal cells are not tightly coupled, the 30–40 μm polytetrafluoroethylene support underlying the basal surface likely reduced the efficiency of the wash, and only a single wash was

performed. Thus, the titers on day 1 likely reflect residual inoculum, rather than de novo virus replication. Taken together, these data suggest that the presence of EBOV GP as a sole envelope protein in the HPIV3 virions resulted in a limited infection of both the apical and basolateral surfaces of HAE, with shedding detectable from the apical surface but not the basolateral surface.

HPIV3/ΔF-HN/EboGP is completely resistant to HPIV3-specific neutralizing antibodies

To determine the susceptibility of HPIV3/ΔF-HN/EboGP to the HPIV3-specific antibodies, we combined 25 μl of Opti-MEM containing 10^4 PFU of HPIV3 or HPIV3/ΔF-HN/EboGP and 10% guinea pig complement with 25 μl of Opti-MEM containing a 1:40 dilution of serum from rabbits that had been hyper-immunized with purified preparations of HPIV3; negative controls contained complement but not serum. The mixtures were incubated for 1 h at 37°C, and residual infectivity was determined by plaque titration. The titers of infectious HPIV3 determined for the samples that contained or lacked HPIV3-neutralizing serum were <2.5 PFU (no residual infectivity detected) and $1.4x10^3$ PFU, respectively, indicating that HPIV3 was completely neutralized by the antibodies, as expected, whereas the control had an approximately 10-fold reduction that might reflect a non-specific effect of the incubation and the presence of complement. In contrast, the titers of HPIV3/ΔF-HN/EboGP from samples that contained or lacked HPIV3-neutralizing serum were $7.0x10^2$ PFU and $5.0x10^2$ PFU, respectively, indicating a lack of sensitivity of the virus to HPIV3-specific antibodies. This also was confirmed during multi-cycle growth in cell culture (not shown), where the inclusion of anti-HPIV3 antibodies in the medium overlay at a dilution of 1:100 completely restricted the replication of HPIV3 with no effect on HPIV3/ΔF-HN/EboGP. In contrast, we previously showed that HPIV3/EboGP is partially sensitive to HPIV3 antibodies in vitro (Bukreyev et al., 2006).

HPIV3/ΔF-HN/EboGP is highly attenuated in vivo

To evaluate HPIV3/ΔF-HN/EboGP replication in vivo, we infected groups of guinea pigs with HPIV3, HPIV3/EboGP, or HPIV3/ΔF-HN/EboGP by the IN route at a dose of $4x10^5$ PFU. On days 2 and 4 post infection, the animals were euthanized, the lungs were isolated and homogenized, and virus titers were determined (Fig. 7). Interestingly, no virus was detected in animals infected with HPIV3/ΔF-HN/EboGP, whereas both HPIV3 and HPIV3/EboGP were readily recoverable, although the titer of the latter virus was reduced by more than 2 $\log_{10}$ compared to HPIV3 on day 2, the peak of virus replication (Fig. 7).

Since HPIV3/ΔF-HN/EboGP was not detected by plaque titration of the lung homogenates, we attempted to detect evidence of infection by immunohistochemical analysis of organs isolated from infected animals. Guinea pigs were infected with HPIV3, HPIV3/EboGP, or HPIV3/ΔF-HN/EboGP by the IN route at a dose of $4x10^5$ PFU. On day 2 after infection, the animals were euthanized and lungs and other organs (listed below) were isolated, fixed in formalin and embedded in paraffin. Tissue sections were prepared and stained with rabbit serum against purified HPIV3 virions, which reacts with various HPIV3 proteins, including the internal proteins (data not shown), and thus would detect the internal proteins of HPIV3/ΔF-HN/EboGP. In animals infected with HPIV3 or HPIV3/EboGP, viral antigen was detected in bronchi and large bronchioles extending into inflammatory alveolar lesions with a moderate amount of antigen in bronchi, and less in smaller airways (Fig. 8A, C, D), as also was observed in a previous study (Yang et al., 2008). With HPIV3/ΔF-HN/EboGP, viral antigen was detected in various parts of the lungs, but the number of cells involved was very low. Fig 8F shows an example of a lung tissue section positive for viral antigen: one focus of positive staining is present in the alveoli, but an adjacent bronchus is negative. In addition, examination of kidneys, liver, thymus, salivary glands, and mediastinal, mesenteric and popliteal lymph nodes revealed no histopathological changes or antigen for any of the three viruses (data not shown). Taken

together, these data confirm the pneumotropism of HPIV3 and HPIV3/EboGP and suggest that HPIV3/ΔF-HN/EboGP is highly attenuated in vivo and did not detectably disseminate beyond the respiratory tract.

Despite the high level of attenuation, HPIV3/ΔF-HN/EboGP is immunogenic

We evaluated the immunogenicity of HPIV3/ΔF-HN/EboGP in comparison with HPIV3/EboGP, for which protective efficacy was previously demonstrated in both guinea pigs and monkeys (Bukreyev et al., 2007; Bukreyev et al., 2006). Groups of guinea pigs were immunized by the IN route with HPIV3 at a dose of $4x10^6$ PFU (Fig. 9, group 7), or HPIV3/EboGP at a dose of $4x10^5$ PFU (group 1), or HPIV3/ΔF-HN/EboGP at a dose of $4x10^5$ or $4x10^6$ PFU (groups 2 and 3), or by the intramuscular (IM) route with HPIV3/ΔF-HN/EboGP at a dose of $4x10^6$ PFU (group 4). The additional groups immunized with HPIV3/ΔF-HN/EboGP at $4x10^6$ PFU were included because, as already noted, the PFU dose of this virus converted to $TCID_{50}$ is 7.3-fold lower than the equal PFU dose of HPIV3/EboGP. To evaluate possible responses due to preformed antigen in the virus inoculum, HPIV3/ΔF-HN/EboGP was inactivated by UV irradiation and additional groups of animals were immunized by the IN or IM route (groups 5 and 6) with the equivalent of $4x10^6$ PFU. Serum samples were collected on days 28 and 56 after immunization and tested for EBOV-specific antibodies by ELISA against inactivated virions (Fig. 9, panel A) and an EBOV neutralization assay (panel B), and for HPIV3-specific antibodies by HAI (panel C).

With regard to EBOV-specific serum ELISA titers (Fig. 9, panel A), administration of HPIV3/ΔF-HN/EboGP by the IN route at doses of $4x10^5$ and $4x10^6$ PFU induced titers of 1:1,100 and 1:1,600, respectively, on day 28 (Fig. 9A, groups 2 and 3, respectively). By day 56, the antibody levels increased further to 1:6,500 and 1:4,600, respectively. These levels are only 2–3 fold lower than that induced by HPIV3/EboGP in the same experiment (3,600 and 13,000 on days 28 and 56, respectively, group 1) despite the highly restricted replication of HPIV3/ΔF-HN/EboGP compared to HPIV3/EboGP. IN inoculation with the UV-inactivated HPIV3/ΔF-HN/EboGP control (group 5) induced little or no response confirming that, while replication of HPIV3/ΔF-HN/EboGP was not detected based on virus titration of lung homogenates (Fig. 7A), the immunogenicity of this virus depended on genome replication. IM immunization with HPIV3/ΔF-HN/EboGP (group 4) induced titers of 1:128 and 1:181 on days 28 and 56, respectively, and thus was substantially less immunogenic than the IN route. However, in a separate experiment (not shown), IM immunization with HPIV3/ΔF-HN/EboGP induced a 6.4-fold greater ($p<0.05$) level of serum ELISA antibodies than IM immunization with HPIV3/EboGP. IM immunization with the UV-inactivated HPIV3/ΔF-HN/EboGP control (group 6) resulted in a low level response.

With regard to EBOV-neutralizing serum antibody titers (Fig. 9B), responses were detected in 5 of the 6 animals immunized with HPIV3/ΔF-HN/EboGP by the IN route at a dose of $4x10^5$ (group 2), in all of the animals immunized by the IN route at a dose of $4x10^6$, and in 3 of 6 animals immunized by the IM route (group 5). The mean antibody titers for these groups paralleled that detected by ELISA. A lack of detectable serum EBOV-neutralizing antibodies, as seen here in some animals, does not necessarily correlate with a lack of protection: we did not evaluate neutralizing titers in our previous studies with HPIV3/EboGP in guinea pigs and rhesus monkeys (Bukreyev et al., 2007;Bukreyev et al., 2006), but a study of vesicular stomatitis virus-vectored EBOV GP in cynomolgus macaques documented complete protection against EBOV challenge in every animal even though neutralizing serum antibodies were undetectable in all animals following vaccination (Jones et al., 2005). With regard to HPIV3 HAI serum antibodies (Fig. 9C), no response was detected in any group immunized with HPIV3/ΔF-HN/EboGP (groups 2–6), as would be expected given the lack of the HN protein.

In a separate experiment, we also evaluated whether prior infection with HPIV3 would reduce the immunogenicity of HPIV3/ΔF-HN/EboGP, a question that we also recently investigated for HPIV3/EboGP (Yang et al., 2008). This might occur, for example, if the HPIV3 internal proteins common to HPIV3 and HPIV3/ΔF-HN/EboGP induced significant protective immunity effective against the latter virus. Also, we tested a lower dose of the vaccine in order to compare the response with that after immunizations with greater doses used in the previous experiments. Guinea pigs were mock-infected (4 animals) or infected (5 animals) IN with $1x10^5$ PFU of HPIV3. Forty-nine days later, serum samples were collected and analyzed for HPIV3-specific HAI antibodies, and all of the animals were infected IN with $4x10^4$ PFU of HPIV3/ΔF-HN/EboGP (Table 1). Twenty eight and 56 days later, serum samples were taken and analyzed for EBOV-specific ELISA serum antibodies. The mean $\log_2$ titers of EBOV-specific antibodies were only slightly (less than 3-fold) reduced in HPIV3-immune group, compared to HPIV3-naive animals, with no statistically significant difference between the two groups at either time point, which is similar to the results that we recently described for HPIV3/EboGP (Yang et al., 2008).

IN immunization with HPIV3/ΔF-HN/EboGP prevents replication and disease from a highly lethal IP EBOV challenge

To evaluate the protective efficacy of HPIV3/ΔF-HN/EboGP, groups of guinea pigs were infected by the IN route with $4x10^5$ PFU of HPIV3, $4x10^5$ PFU of HPIV3/EboGP, or $4x10^6$ PFU of HPIV3/ΔF-HN/EboGP. On day 25 post immunization, the animals were challenged with an otherwise uniformly lethal 1,000 PFU dose of guinea pig-adapted EBOV-Zaire (Connolly et al., 1999) by the IP route. The LD_{50}/PFU ratio of this clone of EBOV is unknown; we note that the values determined for five other guinea pig-adapted strains of EBOV administered by the IP route were >1 (Volchkov et al., 2000), suggesting that, in our case, the IP challenge dose probably exceeded 1,000 LD_{50}. Following challenge, clinical observation and weighing of the animals were performed daily (Fig. 10A). The challenge resulted in weight loss in the HPIV3-immunized control animals starting at day 3, which was followed by the appearance of clinical signs of EBOV infection starting at days 3 – 5 (the clinical scoring is described in the legend to Fig. 10). All the control animals died on days 6, 7, or 8; the one remaining animal was euthanized on day 9 according to the approved animal use protocol due to the severity of the disease. In contrast, animals immunized with HPIV3/EboGP or HPIV3/ΔF-HN/EboGP showed no disease signs, and all the immunized animals survived.

In a separate experiment, guinea pigs were immunized by the IN route with $4x10^5$ PFU of HPIV3 or $4x10^6$ PFU of HPIV3/ΔF-HN/EboGP (four animals per group). On day 28 after immunization, the animals were challenged IP with 1,000 PFU of guinea pig-adapted EBOV as described above. On day 5 following challenge, the animals were euthanized and blood, spleen, liver, and lung samples were collected and analyzed for EBOV by titration. In all of the control HPIV3-immunized animals, high levels of infectious EBOV were detected in all tissues (mean ± SE): in blood, 4.4 ± 0.6 $\log_{10}$ $TCID_{50}$/ml; in spleen, 6.3 ± 0.4 $\log_{10}$ $TCID_{50}$/g; in liver, 6.1 ± 0.2 $\log_{10}$ $TCID_{50}$/g, and in lungs, 4.2 ± 0.4 $\log_{10}$ $TCID_{50}$/g. In contrast, no virus was detected in any tissue of any of the HPIV3/ΔF-HN/EboGP-vaccinated animals. Thus, immunization with HPIV3/ΔF-HN/EboGP conferred solid protection against IP challenge with a uniformly lethal dose of EBOV.

Discussion

We replaced the HN and F proteins of recombinant wild type HPIV3 with the GP of EBOV. This resulted in a viable chimeric virus, HPIV3/ΔF-HN/EboGP, with EBOV GP as its sole surface glycoprotein. Interestingly, HPIV3/ΔF-HN/EboGP retained the general size and shape of an HPIV3 particle, but its envelope thickness and spike morphology resembled those of an

EBOV particle. Even though HPIV3 and EBOV are from different virus families and lack relatedness between the HN and F proteins versus GP, the chimeric virus replicated in LLC-MK2 and Vero monkey kidney cells to titers similar to that of HPIV3. Efficient growth in Vero cells is particularly important, since that provides an acceptable substrate for vaccine manufacture.

We initially anticipated that EBOV GP might not be efficiently incorporated into HPIV3 particles or might not be functional in the foreign envelope. Therefore, we also constructed in parallel a version, called HPIV3/ΔF-HN/EboGPct, in which the CT of EBOV GP was replaced with that of the HPIV3 F protein. This was done to address the possibility that compatibility of the CT of GP with the internal proteins of the HPIV3 particle might be important for the efficient production of infectious particles, as we had previously observed in a study where the HN and F glycoproteins of HPIV3 were replaced with those of HPIV2 (Tao et al., 2000). However, in the present study, this modification reduced rather than increased the efficiency of production of infectious virus and was not further pursued. It may be that, because the EBOV GP and HPIV3 F protein are not significantly related, the chimeric protein created between the two might not have folded correctly or might have functioned suboptimally.

The polarity of viral budding from polarized epithelial cells can greatly affect the pathogenicity of a virus. For example, in Sendai virus, mutations that conferred the ability to bud from the basolateral surface of the respiratory epithelium contributed to systemic disease that was not associated with the wild type virus, which buds from the apical surface (Tashiro et al., 1992). HPIV3, which causes highly localized infections in the respiratory airways, replicates primarily in the apical cells on the luminal surface of the respiratory epithelium, a phenotype that was recapitulated during infection of HAE in vitro as shown here and in previous work (Zhang et al., 2005). In contrast, Marburg virus, a closely related filovirus, is released from the basolateral membranes of infected polarized epithelial cells, even though its GP protein expressed alone or in the context of viral infection is predominately transported to the apical surface (Sanger et al., 2001). The presence of EBOV GP as the sole surface protein in HPIV3/ΔF-HN/EboGP thus had the potential to change the budding phenotype or tissue tropism of the vector. This possibility was investigated here using a well characterized in vitro model of polarized mucocilliary HAE (Pickles et al., 1998). The presence of EBOV GP in HPIV3/EboGP and HPIV3/ΔF-HN/EboGP appeared to confer the ability to infect cells of the basolateral surface when applied directly to that surface, albeit inefficiently, whereas HPIV3 did not detectably infect the basolateral surface. However, expression of EBOV GP did not confer the ability to spread from infected apical cells to underlying cells. Whether HAE were infected on the apical or basolateral surface, virus release from the basolateral surface appeared to be insignificant. In addition, in guinea pigs inoculated by the IN route, the presence of EBOV GP in HPIV3/ΔF-HN/EboGP or HPIV3/EboGP did not result in a detectable systemic infection. The VP40 (matrix) protein of Marburg virus was recently found to contribute to the basolateral budding of the virus by retargeting the GP protein from the apical to the basolateral membrane (Kolesnikova et al., 2007). In the HPIV3 backbone lacking EBOV VP40, this interaction would be lacking and presumably was not supplemented by the internal HPIV3 proteins; indeed, EBOV GP accumulated primarily at the apical surface of HAE. This is consistent with a previous report for Marburg virus (Sanger et al., 2001). Interestingly, the accumulation of GP was localized in the cilia.

Although HPIV3/ΔF-HN/EboGP replicated to high titers in LLC-MK2 and Vero cells, it was highly attenuated in vivo. The high level of immunogenicity of HPIV/ F-HN despite its poor replication compared to HPIV3/EboGP might be due, at least in part, to the formation of GP spikes on the surface HPIV3/ F-HN/EboGP particles (Fig. 2). For example, in the case of the hemagglutinin of avian influenza virus, trimers (which form virion spikes) were more immunogenic than monomers, and multimeric spikes were the most immunogenic form (Wei

et al., 2008). Similarly, the abundant display of GP spikes on HPIV3/ F-HN/EboGP particles compared to their inefficient incorporation into HPIV3/EboGP particles might provide for greater immunogenicity.

Recently, a candidate vaccine virus against EBOV was described based on recombinant vesicular stomatitis virus (VSV) in which the VSV surface glycoprotein G was replaced by GP of EBOV (Garbutt et al., 2004). This vaccine virus replicated 100- to 1000-fold less efficiently than the VSV parent in vitro, although given the high efficiency of replication inherent in the parental VSV backbone, vaccine manufacture would still be feasible. A single IM inoculation of cynomolgus macaques with 10^7 PFU of this VSV-based chimera resulted in a transient viremia in most animals based on virus isolation, did not induce detectable neutralizing serum antibodies in any animal (which became detectable after the challenge), but conferred complete protection in all animals against IM challenge with 1,000 PFU of EBOV (Jones et al., 2005). HPIV3/ΔF-HN/EboGP appeared to be substantially more attenuated than the VSV-based construct based on the lack of recoverable vaccine virus in any of the guinea pigs, an experimental animal that is permissive for HPIV3 and EBOV. Despite this high degree of attenuation, a single dose of $4x10^5$ or $4x10^6$ PFU of HPIV3/ΔF-HN/EboGP induced EBOV-neutralizing serum antibodies in 5 of 6 and 6 of 6 animals, respectively, and was completely protective against an IP EBOV challenge, as already noted. IM immunization with $4x10^6$ PFU of HPIV3/ΔF-HN/EboGP induced EBOV-neutralizing serum antibodies in 3 of 6 animals, indicating that the vaccine was substantially more immunogenic by the IN route. It will be important to extend the evaluation of HPIV3/ΔF-HN/EboGP to non-human primates.

As a candidate vaccine against EBOV, HPIV3/ΔF-HN/EboGP has several advantages over its predecessor, HPIV3/EboGP, which expresses HPIV3 HN and F in addition to EBOV GP as surface proteins. First, HPIV3/ΔF-HN/EboGP had a nearly 2-fold greater incorporation of GP into the particle, as compared to HPIV3/EboGP. This presumably was due to a lack of competition with HN and F for packaging. The absence of HN and F as competing antigens, and the presence of GP in ordered spikes resembling those of a filovirus particle, also might provide for increased immunogenicity. Second, because HPIV3/ΔF-HN/EboGP lacks the HPIV3 HN and F neutralization antigens, it should be more resistant than HPIV3/EboGP to pre-existing immunity against HPIV3. We previously found that, in guinea pigs, immunity to HPIV3 from prior infection completely blocked the replication of a subsequent dose of HPIV3/EboGP (Yang et al., 2008). Interestingly, in this previous study, the HPIV3/EboGP-borne GP retained much of its immunogenicity despite the lack of detectable replication by the vector (Yang et al., 2008), but we note that immunogenicity in HPIV3-immune non-human primates and humans remains to be determined. Thus, HPIV3/ΔF-HN/EboGP provides an alternative should pre-existing immunity to the HPIV3 vector be a problem. Third, HPIV3/ΔF-HN/EboGP is very highly attenuated, as already noted, and thus should be very safe. Taken together, these data provide a strong case for pursuing HPIV3/ΔF-HN/EboGP (in parallel with HPIV3/EboGP) as a vaccine candidate for respiratory immunization against EBOV and warrants testing in non-human primates.

Materials and methods

Design and construction of HPIV3/ΔF-HN/EboGP and HPIV3/ΔF-HN/EboGPct

HPIV3/ΔF-HN/EboGP and HPIV3/ΔF-HN/EboGPct were designed to express complete EBOV GP or EBOV GP bearing the cytoplasmic tail (CT) of HPIV3, respectively, as the sole viral surface protein (Fig. 1A). They were constructed from a previously-described full-length cDNA encoding HPIV3/EboGP (Bukreyev et al., 2006), which consists of the complete HPIV3 backbone in which a transcription cassette containing the ORF for EBOV GP flanked by HPIV3-specific gene-start (GS) and gene-end (GE) transcription signals was inserted between the HPIV3 P and M genes (Fig. 1A). The F and HN genes were deleted from HPIV3/EboGP

as follows (Fig. 1B): First, the construct was modified by insertion of a *Stu*I site into the downstream non-coding region of the HN gene between the open reading frame (ORF) and the gene-end transcriptional signal (Fig. 1B). This was done by replacing the *Xho*I - *Sph*I fragment of the HPIV3/EboGP cDNA (both sites are unique and located at positions 9,519 and 13,339, respectively) with the corresponding fragment from the previously-constructed plasmid p3/7(131)2G-Stu (Durbin et al., 2000), which contains a full-length cDNA of HPIV3 in which three point mutations had been introduced to create the above-mentioned *Stu*I site (Durbin et al., 2000). This replacement resulted in the plasmid HPIV3/EboGP-StuI. Next, we used PCR to amplify and modify nucleotides 5506 – 6899 of HPIV3/EboGP cDNA, a segment that spans the M ORF, so as to introduce a *Stu*I site three nucleotides downstream of the M ORF. This was done using the forward primer ATTTCTTGCTGCAGCGATGG (positions 5506 – 5525 of HPIV3/EboGP) and the reverse primer GAT**AGGCCT**TTACTAGTTCCATTGTTTGA (the underlined sequence in the primer is complementary to the downstream end of the M ORF and the *Stu*I site is in bold). This PCR product was digested with *PflM*1 (an endogenous site present at at nucleotides 5537–5547 in the GP gene of HPIV3/EboGP) and *Stu*I and cloned into the *PflM*I-*Stu*I window of HPIV3/EboGP-StuI. This deleted the F and HN genes and created the full-length HPIV3/ΔF-HN/EboGP cDNA. Construction of the cDNA encoding HPIV3/ΔF-HN/EboGPct, in which the cytoplasmic tail (CT) of the GP protein was replaced with that of HPIV3 F (Fig. 1C), was performed as follows: The pGem-5Zf cloning vector (Promega Inc., Madison, WI) was modified to remove its *Bfu*A1 and *Mlu*1 restriction sites by replacing the *Spe*I-*Nsi*I fragment, containing the two sites, with an irrelevant *Spe*I-*Nsi*I fragment lacking the sites, resulting in the plasmid pGem-5Zf/Spe-Nsi1. Next the *Nco*I-*Nco*I fragment of HPIV3/ΔF-HN/EboGP (positions 3,734–6,252, which includes the downstream end of the EBOV GP gene) was cloned into the unique *Nco*I site of the plasmid pGem-5Zf/SpeI-NsiI, resulting in the plasmid pGem-5Zf/EboGP/NcoI-NcoI. We then amplified the coding sequence for the HPIV3 F gene CT by PCR using primers that added EBOV sequence and cloning sites on either end. The forward primer was GACAATGGATACCG*GCAGGT*ATTGGAGTTACAGGCGTTGTAATTGCAGTTATC GCTTTATTCTGTATATGCAAGTATTACAGAATTCAAAA (the underlined sequence encodes the upstream end of the HPIV3 F CT, the remainder encodes the TM of EBOV GP, and a naturally-occurring *Bfu*AI recognition sequence is italicized) and the reverse primer TCTTAA**ACGCGT**ATTATTTGTTTGTTAGTACAT (the underlined sequence is complementary to that encoding the downstream end of the HPIV3 F CT, the remainder is downstream noncoding sequence from the EBOV GP transcription cassette, and an *Mlu*I site in the latter sequence is in bold). The PCR product was digested with *Mlu*I and *Bfu*AI and the fragment was used to replace the corresponding *Mlu*I-*Bfu*AI fragment of the EBOV GP segment in plasmid pGem-5Zf/EboGP/NcoI-NcoI. This replaced the CT of EBOV GP with that of HPIV3 F, resulting in the plasmid pGem-5zf/EboGP/Nco-Nco-mod. Finally, the *Nco*I-*Nco*I fragment from this plasmid-borne segment was used to replace the corresponding *Nco*I-*Nco*I fragment of HPIV3/ΔF-HN/EboGP, resulting in cDNA encoding HPIV3/ΔF-HN/EboGPct. The modifications in the cDNAs for HPIV3/ΔF-HN/EboGP and HPIV3/ΔF-HN/EboGPct were confirmed by sequence analysis, and recombinant viruses were recovered in cell culture using previously-described methods (Bukreyev et al., 2006). The recombinant HPIV3/ΔF-HN/EboGP virus was amplified by three passages in LLC-MK2 cells at 32ΔC.

Cells, virus amplification and titration and plaque staining

Stocks of HPIV3 and HPIV3/ΔF-HN/EboGP were prepared in LLC-MK2 Rhesus monkey kidney cells (American Type Culture Collection, Manassas, VA) with Opti-MEM medium (Invitrogen, Carlsbad, CA) containing 2.5% fetal bovine serum (Invitrogen). Plaque titration of HPIV3 and HPIV3/ΔF-HN/EboGP was performed as previously described (Bukreyev et al., 2006). In some cases, the $TCID_{50}$ (50% tissue culture infectious dose) titer was determined by

limiting dilution in LLC-MK2 cells. The sensitivity of the viruses to rabbit HPIV3-specific antibodies was evaluated using guinea pig complement (Cambrex Corporation, East Rutherford, NJ), as described in Results. Growth kinetics of the viruses were determined in LLC-MK2 cells, African green monkey kidney Vero cells, and human type II alveolar adenocarcinoma A549 cells (all from the American Type Culture Collection) grown in Opti-MEM medium containing 2.5% fetal bovine serum (Invitrogen). For comparison of plaque morphology, HPIV3 plaques were immunostained with anti-HPIV3 serum as above (Bukreyev et al., 2006), and HPIV3/EboGP and HPIV3/ΔF-HN/EboGP plaques were immunostained in parallel with a 1:1,000 dilution of rabbit antiserum prepared against EBOV that had been inactivated with gamma irradiation (kindly provided by Dr. A. Sanchez, Centers for Control and Prevention, Atlanta, GA).

Electron microscopy

HPIV3 and HPIV3/ΔF-HN/EboGP were purified by centrifugation in 30–60% sucrose step gradients as described previously (Bukreyev et al., 2006). The purified viral particles were bound to 200-mesh Formvar/carbon-coated nickel grids (Electron Microscopy Sciences, Hatfield, PA) and negatively stained with 1% ammonium molybdate. Grids were examined using a model H7500 transmission electron microscope (Hitachi High Technologies, Schaumburg, IL) at 80 kV. The images were obtained with an XR100 digital camera system (Advanced Microscopy Techniques, Danvers, MA).

Polyacrylamide gel electrophoresis, silver staining and Western blotting

Sucrose gradient-purified virus preparations were subjected to polyacrylamide gel electrophoresis under reducing and denaturing conditions using 4–12% gradient NuPAGE gels (Invitrogen). Silver staining was done using the SilverQuest kit (Invitrogen) according the manufacturer's recommendations. Western blotting was performed by conventional methods using a guinea pig antiserum raised by immunization with a DNA vector expressing EBOV GP, which was generously provided by A. Sanchez (Centers for Disease Control and Prevention, Atlanta, GA).

Human airway epithelium (HAE)

Tracheobronchial epithelial cells were obtained from clinical specimens by the University of North Carolina at Chapel Hill Cystic Fibrosis Center Tissue Culture Core under UNC Institutional Review Board-approved protocols. Primary cells were expanded by one passage on Vitrogen-coated plastic dishes, plated at 250,000 cells per 12 mm Millicell culture insert (0.4 μm pore size, Millipore PICM01250), and allowed to differentiate with an air-liquid interface for 4 weeks as previously described (Zhang et al., 2005). For apical inoculation, 2×10^6 PFU of HPIV3, HPIV3/EboGP or HPIV3/ΔF-HN/EboGP in 100 μl of viral suspension (input MOI of 2 PFU/cell) were applied to the apical surface of HAE, cultures were incubated at 37°C for 2 h, the inoculum was removed, apical surfaces were washed twice with 0.5 ml of phosphate buffered saline, and cultures were returned to 37°C. For basolateral inoculations, HAE inserts were inverted, inoculated as above for 2 h, basolateral surfaces were washed one time with 1 ml of phosphate buffered saline, and the inserts were returned to the original orientation. To determine growth kinetics of the viruses, 200 μl aliquots of fresh medium were added to the apical surfaces at specific time points, incubated for 30 min, and harvested as apical wash. Basolateral supernatants were also harvested and replaced with fresh medium. The aliquots were frozen and plaque titrated in LLC-MK2 cells. For identification of the cell types infected by viruses, HAE were fixed with 4% paraformaldehyde, paraffin embedded, and cut into 5 μm sections. Viral antigens were detected with rabbit antiserum against purified HPIV3 or EBOV virions (described above), and Alexafluor-594 (red)-conjugated goat anti-rabbit secondary antibody (Invitrogen). Nuclei were counter-stained with Hoechst 33342 dye

(Invitrogen). Fluorescent confocal images, as well as optical differential interference contrast (DIC) images, were obtained using a Leica SP2 AOBS Upright Laser Scanning Confocal microscope and overlaid images were constructed using Adobe Photoshop software (Adobe Systems, Inc., San Jose, CA).

Inoculation of animals and immunohistochemical analysis of tissues

Guinea pigs (3–4-week-old, strain Hartley, Charles River Laboratories [Wilmington, MA]) were confirmed to be seronegative for HPIV3 by hemagglutinin inhibition (HAI) assay using guinea pig erythrocytes (30). IN inoculation was performed by applying 100 μl of virus suspension in L-15 medium (Invitrogen) into each nostril under mild anesthesia with methoxyflurane (Medical Developments International Limited, Springvale, Australia). For intramuscular (IM) inoculation, 100 μl of the viral suspension was injected into the gastrocnemius muscle under light anesthesia. All procedures with guinea pigs were performed in accordance with protocols and guidelines approved by the NIH Animal Care and Use Committees and were performed in facilities approved by the Association for Assessment and Accreditation of Laboratory Animal Care International. Immunohistochemical analysis of animal tissues was performed as described previously (Yang et al., 2008) using rabbit serum against purified HPIV3 virions, which stains HPIV3/ΔF-HN/EboGP plaques almost as efficiently as HPIV3 or HPIV3/EboGP plaques due to reactivity with both surface and internal HPIV3 proteins (data not shown).

Analysis of antibody responses

EBOV-specific enzyme-linked immunosorbent assay (ELISA) was performed as previously described (Yang et al., 2008) using purified EBOV particles inactivated by gamma-irradiation (kindly provided by Dr. A. Sanchez, Centers for Disease Control and Prevention, Atlanta, GA) as an antigen. EBOV neutralizing antibody titers were determined as previously described (Jahrling, 1999; Jones et al., 2005), except that the endpoint was 60% plaque reduction rather than 80%. HPIV3-specific antibody titers were determined by a hemagglutination inhibition assay (HAI), as described previously (van Wyke Coelingh, Winter, and Murphy, 1985).

EBOV challenge experiments

Experiments involving challenge with EBOV were performed at the biosafety level 4 facility of the Canadian National Microbiology Laboratory. The experiments were approved by the Animal Care Committee of the Canadian Science Centre for Human and Animal Health (Winnipeg, Canada) following the guidelines of the Canadian Council on Animal Care (Ottawa, Canada). Guinea pig adapted EBOV species Zaire, which was produced by serial passages in animals until uniformly lethal (Connolly et al., 1999), was administered by the IP route at a dose of 1,000 PFU. Following challenge, the animals were weighed daily and disease was evaluated using the scoring system described in the legend for Fig. 10. Analysis of EBOV in blood and in internal organs was performed as previously described (Jones et al., 2007). Mean EBOV titers in blood, spleen and liver were determined based on one sample per animal from four animals in each group; viral titers in lungs were determined based on one sample from each lung (i.e., two samples per animal) from four animals per group. In the HPIV3-immunized control group, EBOV was not detected in right lung of one animal; for the purpose of calculation, a titer that was two-fold below the limit of detection was assigned for this negative sample.

Statistical analysis of data

Differences were evaluated by Student's T-test and considered significant when $P<0.05$. Data are shown as means ± SE of the mean.

Acknowledgements

We are grateful to Dr. Anthony Sanchez (Centers for Disease Control and Prevention, Atlanta, Georgia) for providing gamma-irradiated purified EBOV antigen for ELISA, rabbit immune serum against EBOV and guinea pig serum specific for EBOV GP. We thank Ernest Williams and Fatemeh Davoodi for performing HAI assays, Alison Bright and her staff for animal care work and collection of serum samples, and Lawrence J. Faucette and Elizabeth M. Williams for histotechnology assistance. We also thank Jason Gren, National Microbiology Laboratory, Public Health Agency of Canada, for assistance with animal care in high biocontainment. We are grateful to the Directors and teams of the UNC Cystic Fibrosis Center Tissue Culture Core, the Morphology and Morphometry Core and the Michael Hooker Microscopy Facility for supplying reagents and technical expertise and to Susan Burkett for technical assistance. This project was funded as a part of the NIAID Intramural Program, Public Health Agency of Canada, and the National Institutes of Health (NIH) grant NIH R01 HL77844-1.

References

Barouch DH, Pau MG, Custers JH, Koudstaal W, Kostense S, Havenga MJ, Truitt DM, Sumida SM, Kishko MG, Arthur JC, Korioth-Schmitz B, Newberg MH, Gorgone DA, Lifton MA, Panicali DL, Nabel GJ, Letvin NL, Goudsmit J. Immunogenicity of recombinant adenovirus serotype 35 vaccine in the presence of pre-existing anti-Ad5 immunity. J Immunol 2004;172(10):6290–7. [PubMed: 15128818]

Bukreyev A, Rollin PE, Tate MK, Yang L, Zaki SR, Shieh WJ, Murphy BR, Collins PL, Sanchez A. Successful topical respiratory tract immunization of primates against Ebola virus. J Virol 2007;81(12): 6379–88. [PubMed: 17428868]

Bukreyev A, Yang L, Zaki SR, Shieh WJ, Rollin PE, Murphy BR, Collins PL, Sanchez A. A Single Intranasal Inoculation with a Paramyxovirus-Vectored Vaccine Protects Guinea Pigs against a Lethal-Dose Ebola Virus Challenge. J Virol 2006;80(5):2267–79. [PubMed: 16474134]

Casimiro DR, Chen L, Fu TM, Evans RK, Caulfield MJ, Davies ME, Tang A, Chen M, Huang L, Harris V, Freed DC, Wilson KA, Dubey S, Zhu DM, Nawrocki D, Mach H, Troutman R, Isopi L, Williams D, Hurni W, Xu Z, Smith JG, Wang S, Liu X, Guan L, Long R, Trigona W, Heidecker GJ, Perry HC, Persaud N, Toner TJ, Su Q, Liang X, Youil R, Chastain M, Bett AJ, Volkin DB, Emini EA, Shiver JW. Comparative immunogenicity in rhesus monkeys of DNA plasmid, recombinant vaccinia virus, and replication-defective adenovirus vectors expressing a human immunodeficiency virus type 1 gag gene. J Virol 2003;77(11):6305–13. [PubMed: 12743287]

Collins PL, Bukreyev A. Advances in the development of vaccines against Marburg and Ebola viruses. Future Virology 2007;2(6):537–541.

Collins, PL.; Crowe, JEJ. Respiratory Syncytial Virus and Metapneumovirus. In: Knipe, DM.; Howley, PM.; Griffin, DE.; Lamb, RA.; Martin, MA.; Roizman, B.; Straus, SE., editors. Fields Virology. Vol. 5. Vol. 2. Lippincott-Raven Publishers; Philadelphia: 2007. p. 1601-1646.2 vols

Connolly BM, Steele KE, Davis KJ, Geisbert TW, Kell WM, Jaax NK, Jahrling PB. Pathogenesis of experimental Ebola virus infection in guinea pigs. J Infect Dis 1999;179(Suppl 1):S203–17. [PubMed: 9988186]

Durbin AP, Skiadopoulos MH, McAuliffe JM, Riggs JM, Surman SR, Collins PL, Murphy BR. Human parainfluenza virus type 3 (PIV3) expressing the hemagglutinin protein of measles virus provides a potential method for immunization against measles virus and PIV3 in early infancy. J Virol 2000;74 (15):6821–31. [PubMed: 10888621]

Elango N, Coligan JE, Jambou RC, Venkatesan S. Human parainfluenza type 3 virus hemagglutinin-neuraminidase glycoprotein: nucleotide sequence of mRNA and limited amino acid sequence of the purified protein. J Virol 1986;57(2):481–9. [PubMed: 3003381]

Fitzgerald JC, Gao GP, Reyes-Sandoval A, Pavlakis GN, Xiang ZQ, Wlazlo AP, Giles-Davis W, Wilson JM, Ertl HC. A simian replication-defective adenoviral recombinant vaccine to HIV-1 gag. J Immunol 2003;170(3):1416–22. [PubMed: 12538702]

Garbutt M, Liebscher R, Wahl-Jensen V, Jones S, Moller P, Wagner R, Volchkov V, Klenk HD, Feldmann H, Stroher U. Properties of replication-competent vesicular stomatitis virus vectors expressing glycoproteins of filoviruses and arenaviruses. J Virol 2004;78(10):5458–65. [PubMed: 15113924]

Geisbert TW, Pushko P, Anderson K, Smith J, Davis KJ, Jahrling PB. Evaluation in nonhuman primates of vaccines against Ebola virus. Emerg Infect Dis 2002;8(5):503–7. [PubMed: 11996686]

Geisbert TW, Jahrling PB. Exotic emerging viral diseases: progress and challenges. Nat Med 2004;10 (12 Suppl):S110–21. [PubMed: 15577929]

Jaax N, Jahrling P, Geisbert T, Geisbert J, Steele K, McKee K, Nagley D, Johnson E, Jaax G, Peters C. Transmission of Ebola virus (Zaire strain) to uninfected control monkeys in a biocontainment laboratory. Lancet 1995;346(8991–8992):1669–71. [PubMed: 8551825]

Jaax NK, Davis KJ, Geisbert TJ, Vogel P, Jaax GP, Topper M, Jahrling PB. Lethal experimental infection of rhesus monkeys with Ebola-Zaire (Mayinga) virus by the oral and conjunctival route of exposure. Arch Pathol Lab Med 1996;120(2):140–55. [PubMed: 8712894]

Jahrling, PB. Filoviruses and Arenaviruses. In: Murray, PR., editor. Manual of Clinical Microbiology. ASM Press; Washington, D.C: 1999. p. 1125-1136.

Johnson E, Jaax N, White J, Jahrling P. Lethal experimental infections of rhesus monkeys by aerosolized Ebola virus. Int J Exp Pathol 1995;76(4):227–36. [PubMed: 7547435]

Jones SM, Feldmann H, Stroher U, Geisbert JB, Fernando L, Grolla A, Klenk HD, Sullivan NJ, Volchkov VE, Fritz EA, Daddario KM, Hensley LE, Jahrling PB, Geisbert TW. Live attenuated recombinant vaccine protects nonhuman primates against Ebola and Marburg viruses. Nat Med 2005;11(7):786–790. [PubMed: 15937495]

Jones SM, Stroher U, Fernando L, Qiu X, Alimonti J, Melito P, Bray M, Klenk HD, Feldmann H. Assessment of a vesicular stomatitis virus-based vaccine by use of the mouse model of Ebola virus hemorrhagic fever. J Infect Dis 2007;196(Suppl 2):S404–12. [PubMed: 17940977]

Kanesa-Thasan N, Smucny JJ, Hoke CH, Marks DH, Konishi E, Kurane I, Tang DB, Vaughn DW, Mason PW, Shope RE. Safety and immunogenicity of NYVAC-JEV and ALVAC-JEV attenuated recombinant Japanese encephalitis virus-poxvirus vaccines in vaccinia-nonimmune and vaccinia-immune humans. Vaccine 2000;19(4–5):483–91. [PubMed: 11027812]

Karron, RA.; Collins, PL. Parainfluenza Viruses. In: Knipe, DM.; Howley, PM.; Griffin, DE.; Lamb, RA.; Martin, MA.; Roizman, B.; Straus, SE., editors. Fields Virology. Vol. 5. Lippincott-Raven Publishers; Philadelphia: 2007. p. 12 vols

Kolakofsky D, Pelet T, Garcin D, Hausmann S, Curran J, Roux L. Paramyxovirus RNA Synthesis and the Requirement for Hexamer Genome Length: the Rule of Six Revisited. J Virol 1998;72(2):891–9. [PubMed: 9444980]

Kolesnikova L, Ryabchikova E, Shestopalov A, Becker S. Basolateral budding of Marburg virus: VP40 retargets viral glycoprotein GP to the basolateral surface. J Infect Dis 2007;196(Suppl 2):S232–6. [PubMed: 17940954]

Lemckert AA, Sumida SM, Holterman L, Vogels R, Truitt DM, Lynch DM, Nanda A, Ewald BA, Gorgone DA, Lifton MA, Goudsmit J, Havenga MJ, Barouch DH. Immunogenicity of heterologous prime-boost regimens involving recombinant adenovirus serotype 11 (Ad11) and Ad35 vaccine vectors in the presence of anti-ad5 immunity. J Virol 2005;79(15):9694–701. [PubMed: 16014931]

Pickles RJ, McCarty D, Matsui H, Hart PJ, Randell SH, Boucher RC. Limited entry of adenovirus vectors into well-differentiated airway epithelium is responsible for inefficient gene transfer. J Virol 1998;72 (7):6014–23. [PubMed: 9621064]

Sanchez, A.; Geisbert, TW.; Feldmann, H. Filoviridae: Marburg and Ebola Viruses. In: Knipe, DM.; Howley, PM.; Griffin, DE.; Lamb, RA.; Martin, MA.; Roizman, B.; Straus, SE., editors. Fields Virology. Vol. 5. Lippincott-Raven Publishers; Philadelphia: 2007. p. 12 vols

Sanchez A, Kiley MP, Holloway BP, Auperin DD. Sequence analysis of the Ebola virus genome: organization, genetic elements, and comparison with the genome of Marburg virus. Virus Res 1993;29(3):215–40. [PubMed: 8237108]

Sanchez A, Trappier SG, Mahy BW, Peters CJ, Nichol ST. The virion glycoproteins of Ebola viruses are encoded in two reading frames and are expressed through transcriptional editing. Proc Natl Acad Sci U S A 1996;93(8):3602–7. [PubMed: 8622982]

Sanger C, Muhlberger E, Ryabchikova E, Kolesnikova L, Klenk HD, Becker S. Sorting of Marburg virus surface protein and virus release take place at opposite surfaces of infected polarized epithelial cells. J Virol 2001;75(3):1274–83. [PubMed: 11152500]

Sharpe S, Polyanskaya N, Dennis M, Sutter G, Hanke T, Erfle V, Hirsch V, Cranage M. Induction of simian immunodeficiency virus (SIV)-specific CTL in rhesus macaques by vaccination with

modified vaccinia virus Ankara expressing SIV transgenes: influence of pre-existing anti-vector immunity. J Gen Virol 2001;82(Pt 9):2215–23. [PubMed: 11514732]

Spriggs MK, Olmsted RA, Venkatesan S, Coligan JE, Collins PL. Fusion glycoprotein of human parainfluenza virus type 3: nucleotide sequence of the gene, direct identification of the cleavage-activation site, and comparison with other paramyxoviruses. Virology 1986;152(1):241–51. [PubMed: 3012869]

Storey DG, Dimock K, Kang CY. Structural characterization of virion proteins and genomic RNA of human parainfluenza virus 3. J Virol 1984;52(3):761–6. [PubMed: 6092708]

Sumida SM, Truitt DM, Kishko MG, Arthur JC, Jackson SS, Gorgone DA, Lifton MA, Koudstaal W, Pau MG, Kostense S, Havenga MJ, Goudsmit J, Letvin NL, Barouch DH. Neutralizing antibodies and CD8+ T lymphocytes both contribute to immunity to adenovirus serotype 5 vaccine vectors. J Virol 2004;78(6):2666–73. [PubMed: 14990686]

Tao T, Skiadopoulos MH, Davoodi F, Riggs JM, Collins PL, Murphy BR. Replacement of the ectodomains of the hemagglutinin-neuraminidase and fusion glycoproteins of recombinant parainfluenza virus type 3 (PIV3) with their counterparts from PIV2 yields attenuated PIV2 vaccine candidates. J Virol 2000;74(14):6448–58. [PubMed: 10864657]

Tashiro M, Seto JT, Choosakul S, Yamakawa M, Klenk HD, Rott R. Budding site of Sendai virus in polarized epithelial cells is one of the determinants for tropism and pathogenicity in mice. Virology 1992;187(2):413–22. [PubMed: 1312267]

van Wyke Coelingh KL, Winter C, Murphy BR. Antigenic variation in the hemagglutinin-neuraminidase protein of human parainfluenza type 3 virus. Virology 1985;143(2):569–82. [PubMed: 2414910]

Volchkov VE, Becker S, Volchkova VA, Ternovoj VA, Kotov AN, Netesov SV, Klenk HD. GP mRNA of Ebola virus is edited by the Ebola virus polymerase and by T7 and vaccinia virus polymerases. Virology 1995;214(2):421–30. [PubMed: 8553543]

Volchkov VE, Chepurnov AA, Volchkova VA, Ternovoj VA, Klenk HD. Molecular characterization of guinea pig-adapted variants of Ebola virus. Virology 2000;277(1):147–55. [PubMed: 11062045]

Wechsler SL, Lambert DM, Galinski MS, Pons MW. Intracellular synthesis of human parainfluenza type 3 virus-specified polypeptides. J Virol 1985;54(3):661–4. [PubMed: 2987519]

Wei CJ, Xu L, Kong WP, Shi W, Canis K, Stevens J, Yang ZY, Dell A, Haslam SM, Wilson IA, Nabel GJ. Comparative efficacy of neutralizing antibodies elicited by recombinant hemagglutinin proteins from avian H5N1 influenza virus. J Virol 2008;82(13):6200–8. [PubMed: 18417563]

Wright PF, Ikizler MR, Gonzales RA, Carroll KN, Johnson JE, Werkhaven JA. Growth of respiratory syncytial virus in primary epithelial cells from the human respiratory tract. J Virol 2005;79(13):8651–4. [PubMed: 15956607]

Yang L, Sanchez A, Ward JM, Murphy BR, Collins PL, Bukreyev A. A paramyxovirus-vectored intranasal vaccine against Ebola virus is immunogenic in vector-immune animals. Virology. 2008**In press.**(VIRO-07–897)

Yang ZY, Wyatt LS, Kong WP, Moodie Z, Moss B, Nabel GJ. Overcoming immunity to a viral vaccine by DNA priming before vector boosting. J Virol 2003;77(1):799–803. [PubMed: 12477888]

Zhang L, Bukreyev A, Thompson CI, Watson B, Peeples ME, Collins PL, Pickles RJ. Infection of ciliated cells by human parainfluenza virus type 3 in an in vitro model of human airway epithelium. J Virol 2005;79(2):1113–24. [PubMed: 15613339]

Zhi Y, Figueredo J, Kobinger GP, Hagan H, Calcedo R, Miller JR, Gao G, Wilson JM. Efficacy of Severe Acute Respiratory Syndrome Vaccine Based on a Nonhuman Primate Adenovirus in the Presence of Immunity Against Human Adenovirus. Hum Gene Ther 2006;17(5):500–6. [PubMed: 16716107]

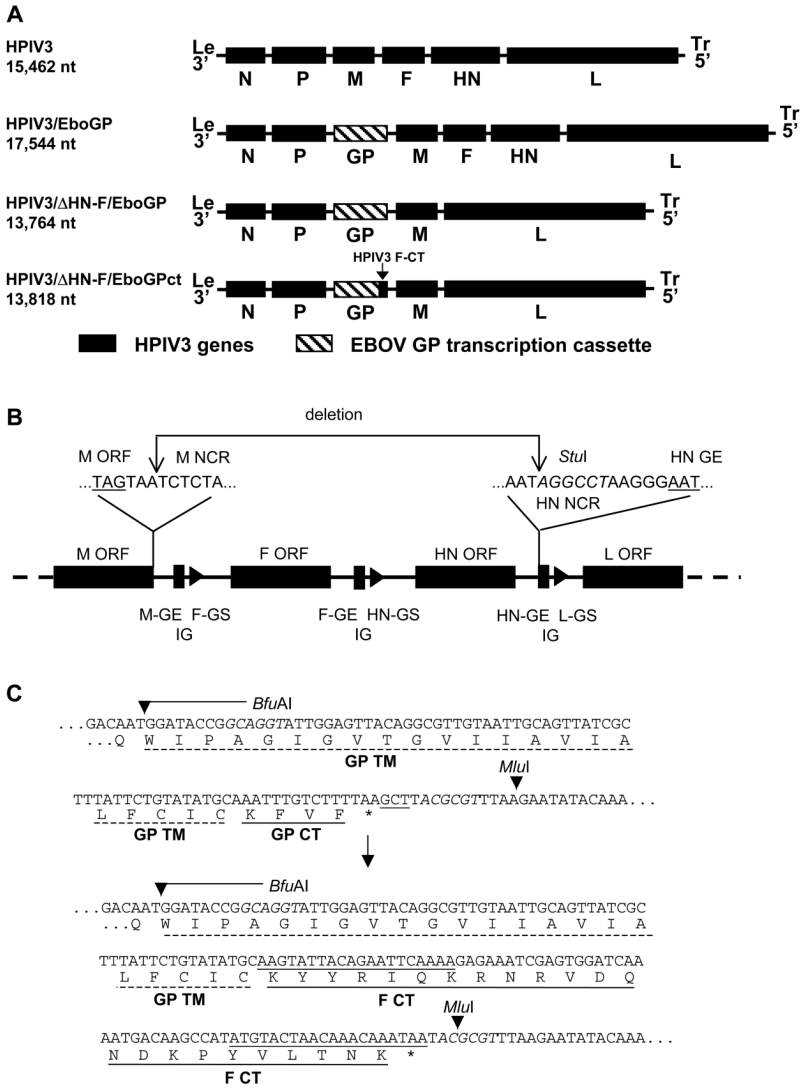

Fig. 1.

Construction of HPIV3/ΔF-HN/EboGP, expressing the complete EBOV GP, and HPIV3/ΔF-HN/EboGPct, expressing EBOV GP bearing the cytoplasmic tail (CT) of the HPIV3 F protein. **A**. Genome maps of, in descending order: complete infectious HPIV3; HPIV3/EboGP, which was previously derived (Bukreyev et al., 2007; Bukreyev et al., 2006) from HPIV3 by insertion, between the HPIV3 P and M genes, of a transcription cassette expressing the complete EBOV GP; HPIV3/ΔF-HN/EboGP, which was derived from HPIV3/EboGP by deleting the HPIV3 F and HN genes; and HPIV3/ΔF-HN/EboGPct, which was derived from HPIV3/ΔF-HN/EboGP by replacing the CT of EBOV GP with that of HPIV3 F. The genome nucleotide lengths are shown to the left. **B.** Deletion of HPIV3 F and HN genes. The region of the HPIV3/EboGP genome spanning the M, F, HN, and L genes is shown; ORFs are indicated as filled rectangles that are flanked by horizontal lines indicating noncoding gene regions; gene junctions are indicated as a filled bar denoting a gene-end (GE) signal, a short horizontal line denoting an intergenic (IG) trinucleotide, and a filled arrowhead denoting a gene-start (GS) signal. The sequences at the deletion points are expanded above the diagram. A *Stu*I site that was introduced 6–11 nucleotides upstream of the HN GE signal is italicized. The deletion begins at the fourth nucleotide following the M ORF and ends at the above-mentioned *Stu*I site. **C.** Replacement

of the CT of EBOV GP with that of HPIV3 F. Top: the downstream part of EBOV GP is shown with the transmembrane domain (TM) and the CT indicated by dashed and solid lines, respectively. Bottom: modified chimeric GP in which the GP CT has been replaced with the much longer CT from HPIV3 F. The stop codon is depicted with an asterisk. *Bfu*AI and *Mlu*I recognition sequences present in the EBOV GP transcription cassette and used for the replacement are italicized with their cleavage sites indicated with arrowheads (note that *Bfu*AI cuts outside of, and in this case upstream of, its recognition sequence).

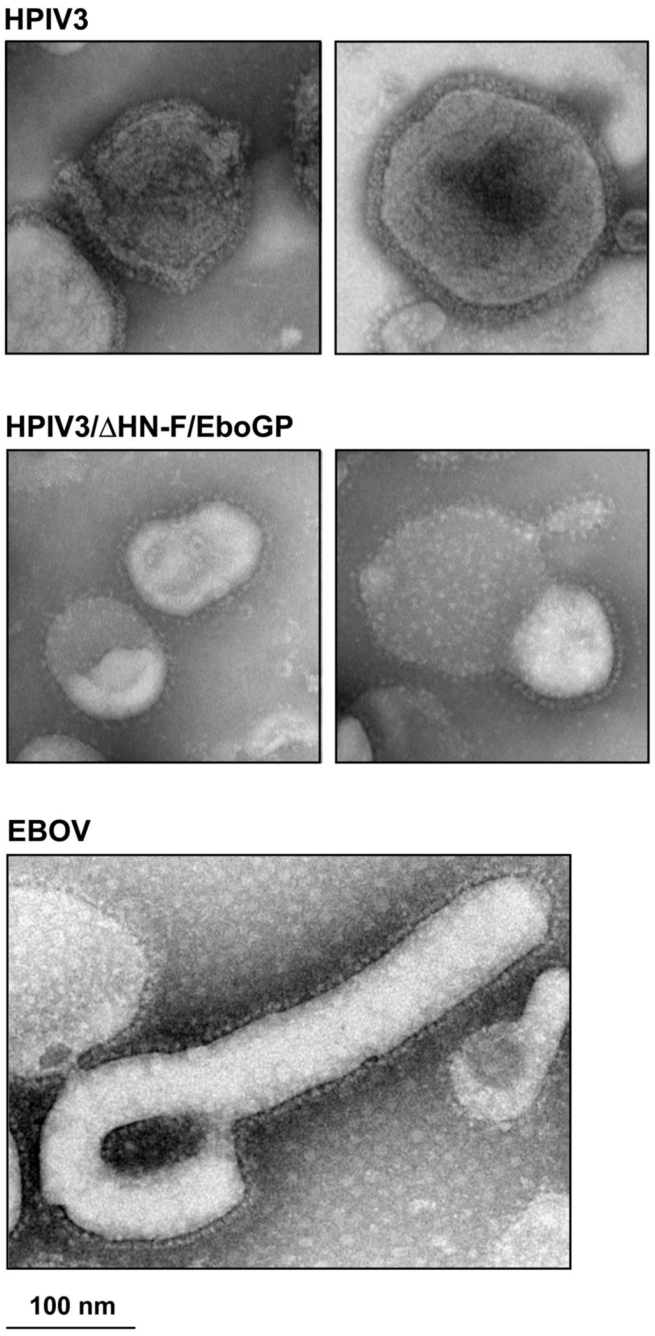

Fig. 2.

Electron micrographs of negative-stained particles of HPIV3, HPIV3/ΔF-HN/EboGP, and EBOV. Note that the envelope of HPIV3/ΔF-HN/EboGP is thinner than that of HPIV3 and contains spikes that resemble those of EBOV rather than HPIV3. Conversely, the shape of the HPIV3/ΔF-HN/EboGP particle resembles that of HPIV3 rather than EBOV. The EBOV image was kindly provided by C. Humphrey and A. Sanchez (Centers for Disease Control and Prevention, Atlanta, GA).

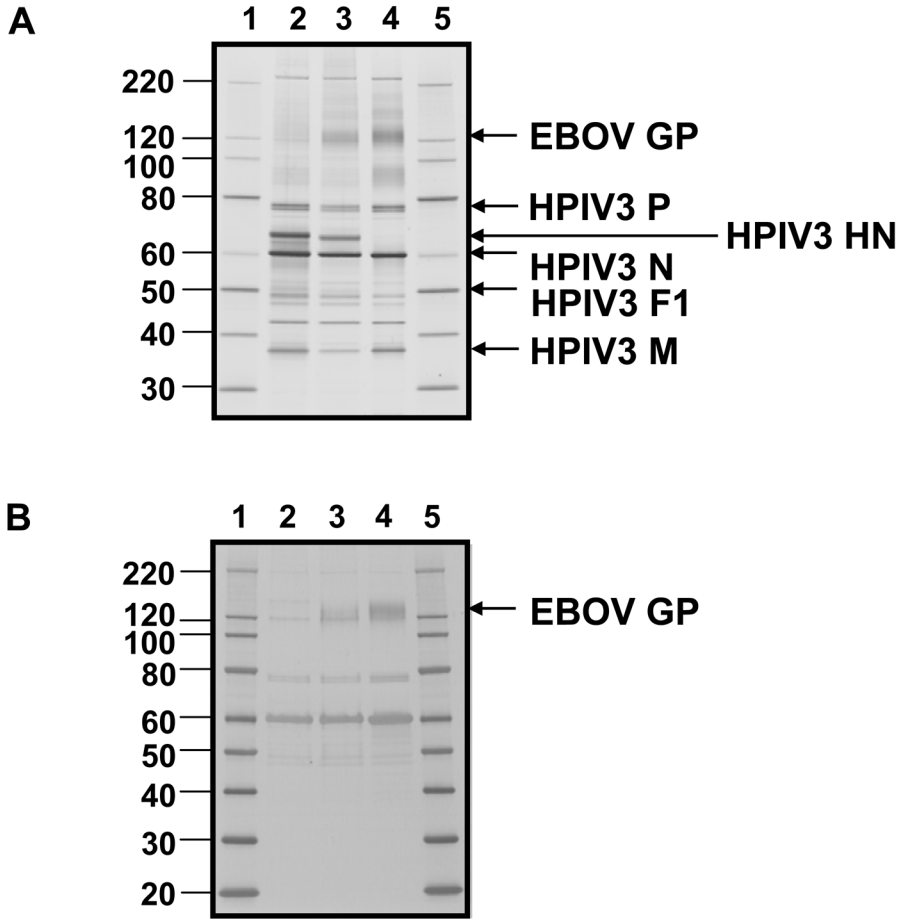

Fig. 3.

Analysis of purified virions of HPIV3, HPIV3/EboGP, and HPIV3/ΔF-HN/EboGP by gel electrophoresis in conjunction with silver staining (A) or Western blotting using a guinea pig antiserum raised against a DNA vaccine expressing EBOV GP (B). Lanes: 1 and 5, MagicMark XP (Invitrogen) with the corresponding molecular weights indicated to the left; 2, HPIV3; 3, HPIV3/EboGP; 4, HPIV3/ΔF-HN/EboGP. The HPIV3 P, HN, N, F1 and M bands are identified based on published profiles (Storey, Dimock, and Kang, 1984; Wechsler et al., 1985) and the position of EBOV GP is indicated.

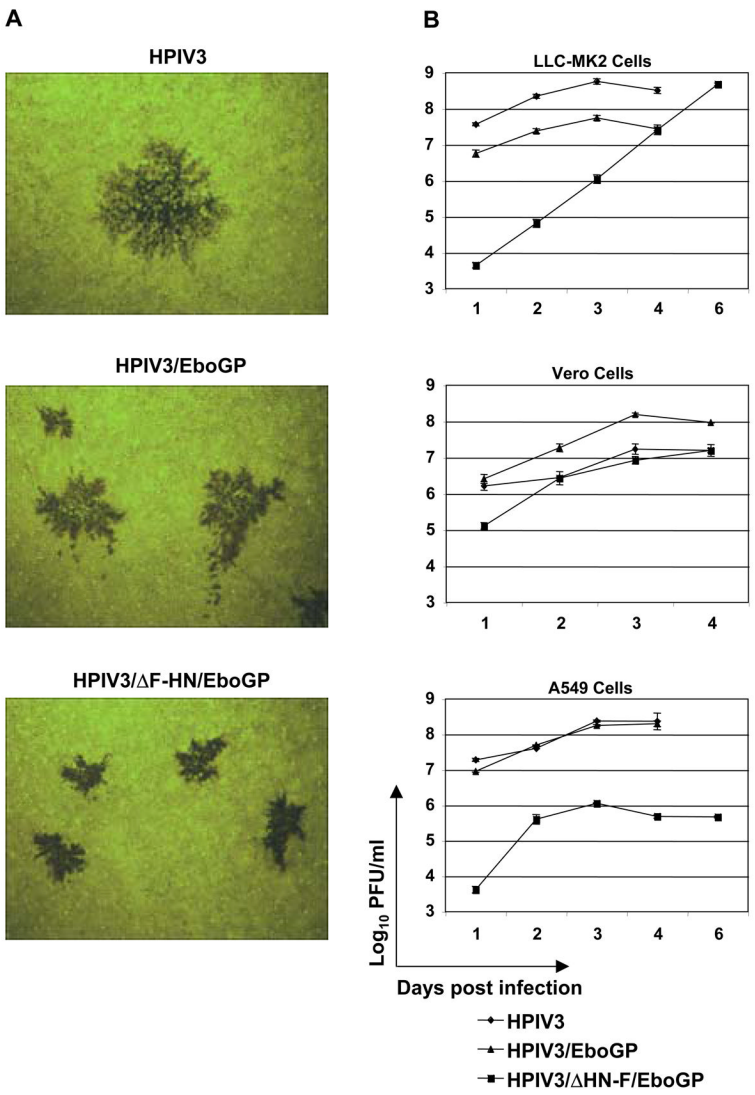

Fig. 4.

Replication of HPIV3/ΔF-HN/EboGP in cell monolayers. **A.** Plaque formation in LLC-MK2 cells by HPIV3, HPIV3/EboGP and HPIV3/ΔF-HN/EboGP. The cells were incubated under methycellulose for 6 days at 32°C, fixed, and analyzed immunostaining with rabbit antiserum rraised against purified HPIV3 virions (HPIV3 panel) or purified inactivated EBOV virions (HPIV3/EboGP and HPIV3/ΔF-HN/EboGP panels). **B.** Growth kinetics of HPIV3, HPIV3/EboGP and HPIV3/ΔF-HN/EboGP in LLC-MK2, Vero and A549 cells. Cells were infected at an MOI of 3 PFU/cell during a 2-h adsorption period, washed three times, and incubated at 32°C. Aliquots of the overlying medium were taken on days 1, 2, 3, 4, and 6 and replaced with fresh medium. Viral titers in the aliquots were determined by plaque titration in LLC-MK2 cells. Mean values ± SE, based on three monolayers per virus, are shown. The limit of detection is 1.7 $\log_{10}$ PFU/ml, with the exception of day 1, for which it was 0.7 $\log_{10}$ PFU/ml. Note that for many time points, error bars cannot be seen due to the low variability. In LLC-MK2 and A549 cells infected with HPIV3 and HPIV3/EboGP, the monolayers were completely destroyed by day 6, and therefore medium aliquots were not collected. Data from one of the two independent experiments performed are shown. Growth kinetics of HPIV3 and HPIV3/

EboGP in LLC-MK2 and Vero cells using low MOI (0.001 PFU) were determined in a previous study (Bukreyev et al., 2006).

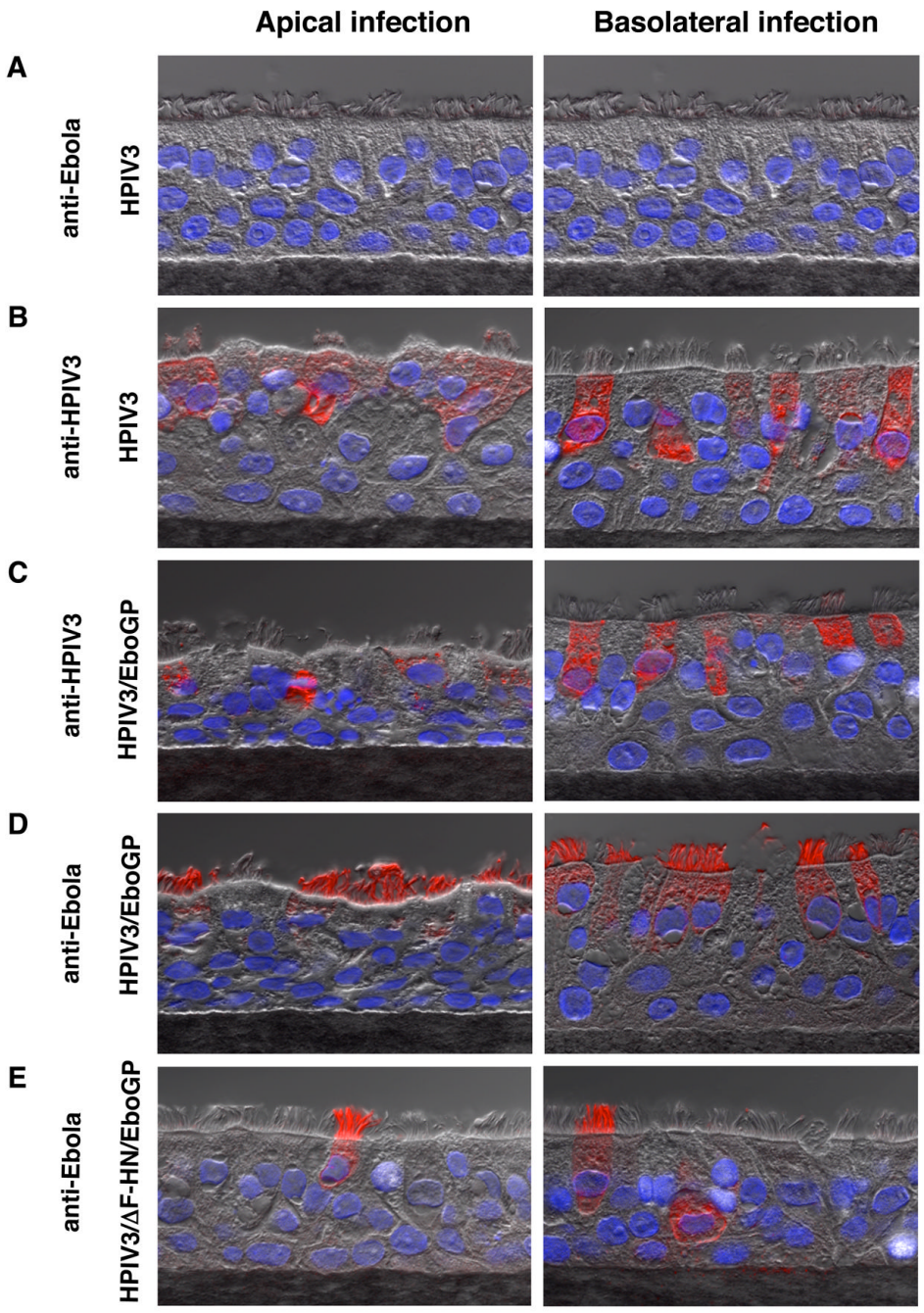

Fig. 5.

Infection of an in vitro model of human airway epithelium (HAE) with HPIV3 (rows A and B), HPIV3/EboGP (rows C and D), and HPIV3/ΔF-HN/EboGP (row E): selected representative cross-sectional images. HAE were inoculated from either the apical (left column) or basolateral surface (right column; note that the method used for basolateral inoculation exposed both surfaces to infection, see the text), and were fixed and analyzed by immunostaining on day 2 (HPIV3/EboGP) or day 4 (HPIV3, HPIV3/ΔF-HN/EboGP). Viral antigen was detected with rabbit antiserum raised against purified HPIV3 virions (rows B and C) or purified, inactivated EBOV virions (rows A, D and E) as the first antibody followed by a labeled second antibody (red), and the nuclei were stained blue with DAPI. Treatment of

HPIV3-infected HAE with the EBOV-specific antibodies did not result in antigen detection, as expected (row A). Specificity of stainings was also established in preliminary experiments (data not shown).

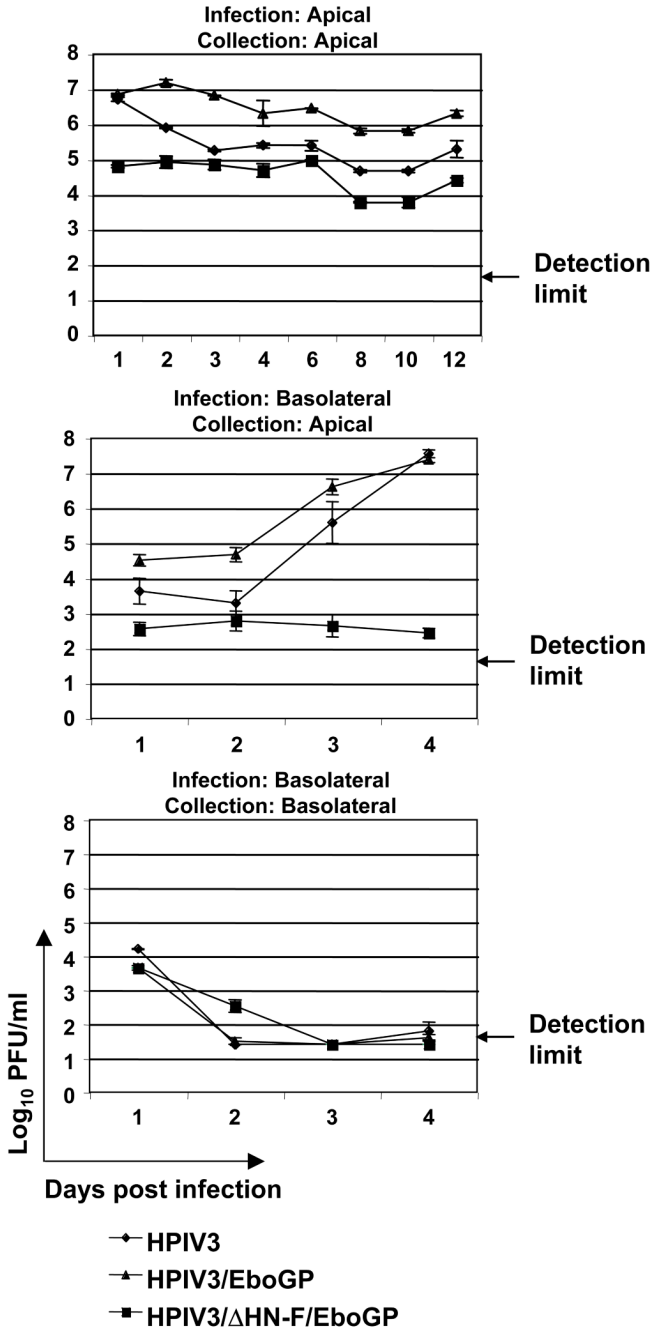

Fig. 6.

Growth kinetics of HPIV3, HPIV3/EboGP and HPIV3/ΔF-HN/EboGP on HAE. Triplicate HAE cultures were inoculated with viruses at an MOI of 2 PFU via the apical or basolateral and apical surfaces, viral supernatants from the apical or basolateral compartments were harvested, and viral titers were determined by plaque titration in LLC-MK2 cells. Means represent three samples per group ± SE. For the samples below the limit of detection, which was 1.7 $\log_{10}$ PFU/ml, the value two-fold below the limit (1.4 $\log_{10}$ PFU/ml) was assigned for calculation of the means.

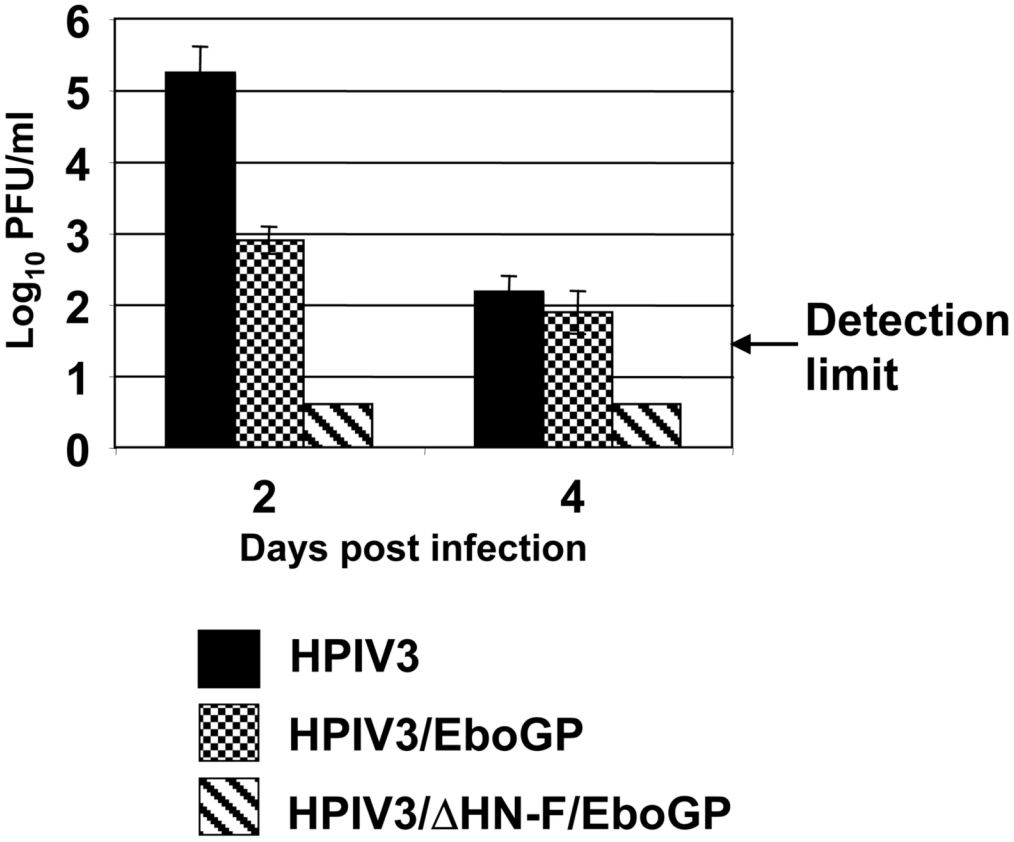

Fig. 7.

Replication of HPIV3, HPIV3/EboGP and HPIV3/ΔF-HN/EboGP in the lungs of guinea pigs: virus titers in the lungs harvested on days 2 and 4 after IN infection at a dose of $4X10^5$ PFU per animal. Mean values ± SE are based on five (HPIV3) or six (HPIV3/EboGP, HPIV3/ΔF-HN/EboGP) animals per time point. No infectious HPIV3/ΔF-HN/EboGP was recovered at either time point (level of detection 1.47 $\log_{10}$ PFU/g).

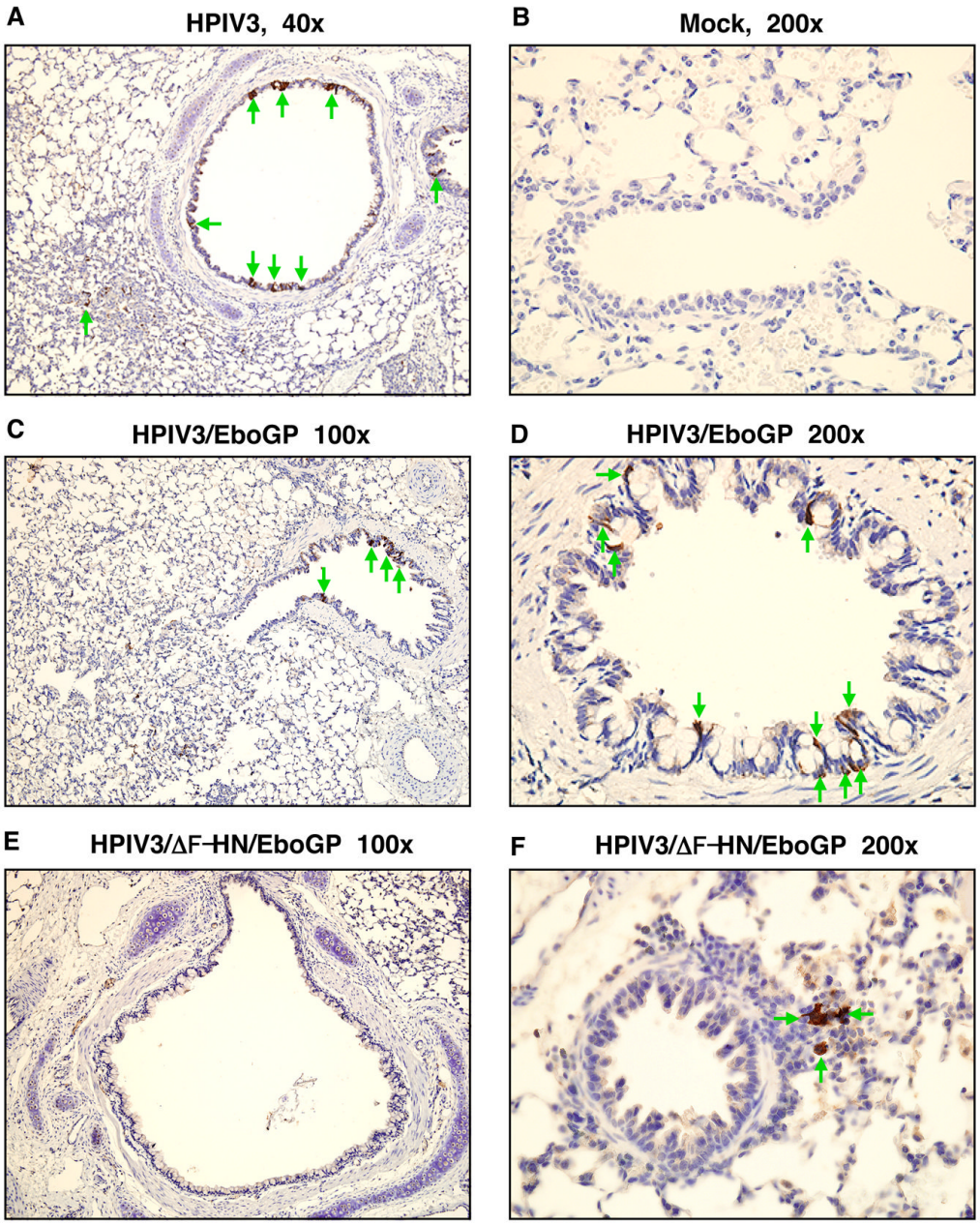

Fig. 8.

Immunohistochemical analysis of viral antigen distribution in guinea pig lungs on day 2 after IN infection with $4x10^5$ PFU of HPIV3 (**A**), HPIV3/EboGP (**C, D**), HPIV3/ΔF-HN/EboGP (**E, F**), or mock infection (**B**). **A**, **C**, **D**, Viral antigen detected in bronchial epithelium. **F**, A focus of positive staining present in alveoli; an adjacent bronchiole is negative. **E**, Lack of viral antigen in a bronchus. Viral antigen is stained brown against a background of hematoxylin counterstain; cells positive for the antigen are shown with green arrows.

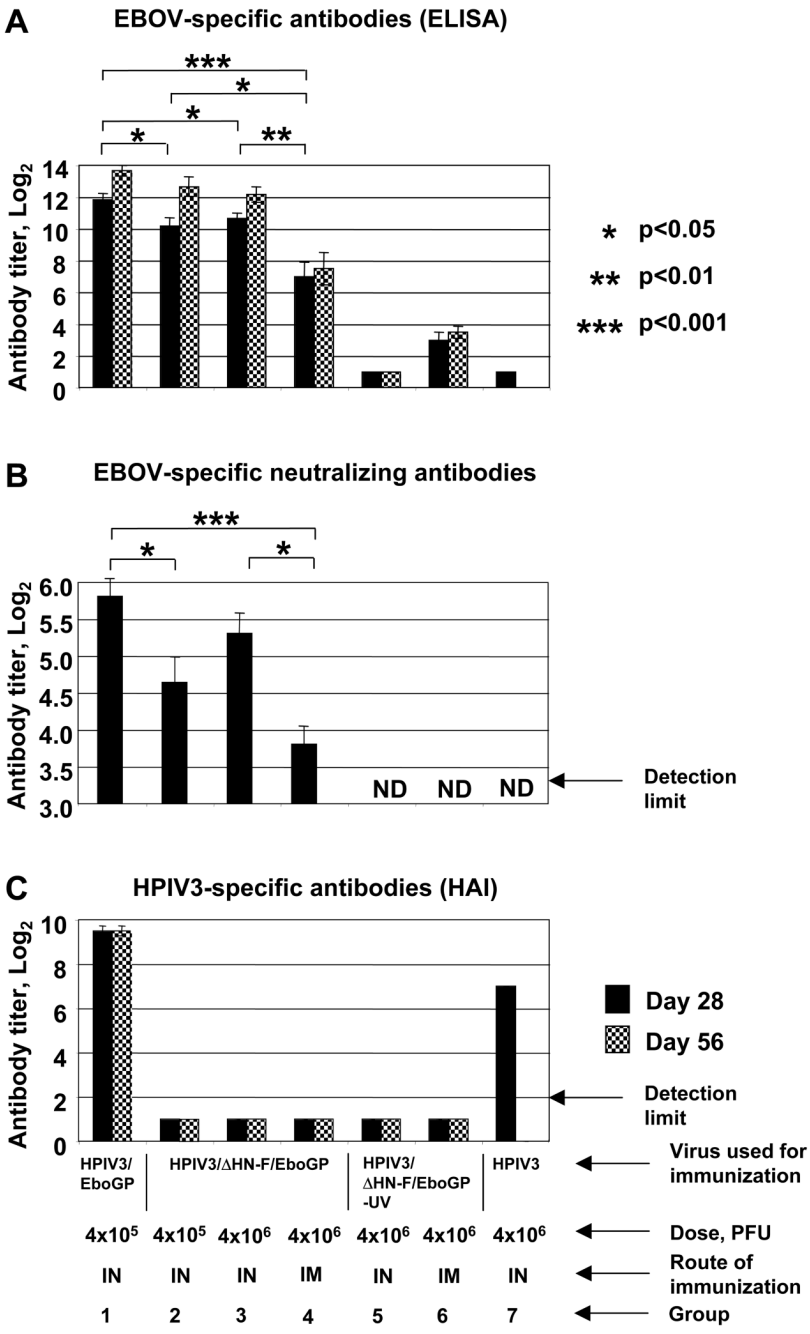

Fig. 9.

Serum antibody responses in guinea pigs 28 (filled bars) and 56 (cross-hatched bars) days following inoculation with $4x10^5$ PFU of HPIV3/EboGP given IN (group 1), $4x10^5$ or $4x10^6$ PFU of HPIV3/ΔF-HN/EboGP given IN (groups 2 and 3), $4x10^6$ PFU of HPIV3/ΔF-HN/EboGP given IM (group 4), the equivalent of $4x10^6$ PFU of UV-inactivated HPIV3/ΔF-HN/EboGP given IN (group 5) or IM (group 6), and $4x10^6$ PFU of HPIV3 given IN (group 7). **A**, EBOV-specific antibody titers, determined by ELISA against inactivated EBOV particles. **B,** EBOV-specific 60% plaque reduction titers (day 28 only); 1 of 6 animals in group 2 and 3 of 6 animals in group 4 lacked detectable neutralizing antibodies and were assigned values of 1:10 for the purpose of calculation. **C**, HPIV3-specific antibody titers, determined by HAI; the

samples from groups 2–6 were below the limit of detection and were assigned values of 1:20 for the purpose of calculation. Results from all three assays are expressed as mean values ± SE based on six animals per groups 1–4, four animals per groups 5 and 6, and two animals per group 7 (this last group was from a separate experiment that was included for comparison; mean with no SE). The differences between the groups 1 and 3 in the levels of the EBOV-specific ELISA (A) and neutralizing (B) antibody responses are not significant with the exception of the ELISA titers on day 56, for which the difference is significant ($p<0.05$). ND, not done. A second experiment with additional animals yielded similar results (not shown). Statistical significances of differences between the values for groups 1–4 are shown in panel A (day 28 only) and panel B.

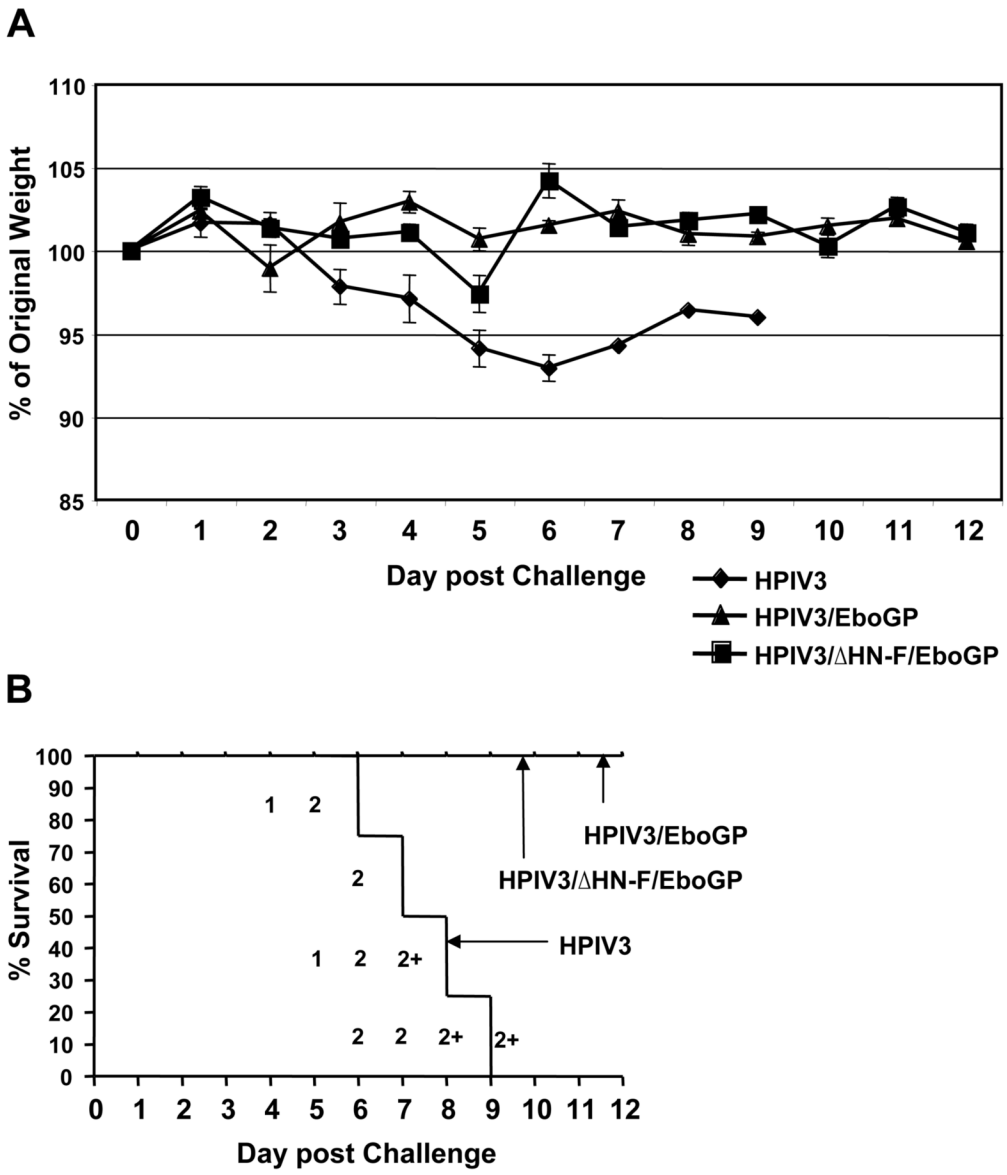

Fig. 10.

Challenge with EBOV: guinea pigs were immunized IN with $4x10^5$ PFU of HPIV3 (4 animals), $4x10^5$ PFU of HPIV3/EboGP (4 animals), or $4x10^6$ PFU of HPIV3/ΔF-HN/EboGP (6 animals), and challenged 25 days later with 1,000 PFU of EBOV by the IP route. **A.** Percent change in body weight following EBOV challenge. Daily mean weights ± SE are shown expressed as a percentage of the weight on day 0. When one or more animals in a group died, the SE was calculated based on the remaining live animals, with a minimum of 3 animals per group. **B**. Kaplan-Maier survival curves and clinical disease scores. All of the animals immunized with HPIV3/ΔF-HN/EboGP or HPIV3/EboGP survived, while all of the HPIV3-immunized (control) animals died. Disease signs were observed only in the control group and were scored daily for each of the four animals as follows: 1, ruffled fur, reduced activity, loss of body conditions; 2, labored breathing, hunched posture, bleeding, marked lethargy; 2+, same as 2, but extremely severe. Each row represents the daily scores for one of the four control animals in that group, ending with a vertical line on the day of death. One animal shown in the bottom was euthanized on day 9 due to severity of the disease.

Table 1

Immunogenicity of HPIV3/ΔF-HN/EboGP in HPIV3-immune and HPIV3-naïve guinea pigs.

Groups[a]	Titer of HPIV3- specific HAI serum antibodies (day 49)[a]	Titer of EBOV-specific serum ELISA antibodies following administration of HPIV3/ΔF-HN/EboGP on day 49[b]	
		Day 77	Day 105
HPIV3-naïve	< 2	8.0 ± 0.8	10.0 ± 0.4
HPIV3-immune	10.5 ± 1.0	6.5 ± 0.5	8.5 ± 0.6

[a] On day 0, animals were mock-infected (4 animals, HPIV3-naïve group) or infected IN with $1x10^5$ PFU of HPIV3 (5 animals, HPIV3-immune group). Serum samples were taken on day 49 and analyzed for HPIV3-specific antibodies by HAI assay. These are expressed as mean reciprocal $\log_2$ titers ± SE.

[b] On day 49, both groups were immunized IN with $4x10^4$ PFU of HPIV3/ΔF-HN/EboGP. Twenty-eight and 56 days later (days 77 and 105, respectively), serum samples were taken and assayed by ELISA against inactivated EBOV. Titers are expressed as mean reciprocal $\log_2$ titers ± SE. Background titers in sera from animals not immunized with HPIV3/ΔF-HN/EboGP and analyzed in parallel were < 2 $\log_2$.